Copyright Warning & Restrictions

The copyright law of the United States (Title 17, United States Code) governs the making of photocopies or other reproductions of copyrighted material.

Under certain conditions specified in the law, libraries and archives are authorized to furnish a photocopy or other reproduction. One of these specified conditions is that the photocopy or reproduction is not to be "used for any purpose other than private study, scholarship, or research." If a, user makes a request for, or later uses, a photocopy or reproduction for purposes in excess of "fair use" that user may be liable for copyright infringement,

This institution reserves the right to refuse to accept a copying order if, in its judgment, fulfillment of the order would involve violation of copyright law.

Please Note: The author retains the copyright while the New Jersey Institute of Technology reserves the right to distribute this thesis or dissertation

Printing note: If you do not wish to print this page, then select "Pages from: first page # to: last page #" on the print dialog screen

67-14,248

LURIE, Michael Jay, 1939-
EFFECTS OF PARTIAL COHERENCE ON HOLOGRAPHY.

Newark College of Engineering, D. Eng. Sc., 1967
Engineering, electrical

University Microfilms, Inc., Ann Arbor, Michigan

EFFECTS OF PARTIAL COHERENCE ON HOLOGRAPHY

BY

MICHAEL (JAY) LURIE

A DISSERTATION

PRESENTED IN PARTIAL FULFILLMENT OF

THE REQUIREMENTS FOR THE DEGREE

OF

DOCTOR OF ENGINEERING SCIENCE

AT

NEWARK COLLEGE OF ENGINEERING

Newark, New Jersey
1967

ABSTRACT

The theory of two-beam holography is generalized to include quasi-monochromatic radiation of any degree of spatial coherence. It is shown that a clear, undistorted reconstruction can be obtained provided the reference beam is highly coherent. The effect of the partial coherence of the illumination is only to make the reconstructed image darker. Specifically, the amplitude of the radiation at any point of the image is proportional to the amplitude of the radiation leaving the corresponding point on the object during the exposure, times the magnitude of the coherence between the latter radiation and the reference beam. Holograms made using either a plane or a spherical reference beam are discussed in detail.

A technique is developed for measuring the magnitude of the degree of coherence of the radiation at every point on the object surface, with respect to the reference beam, by measuring the irradiance at the real image reconstruction of the object. As an example, the coherence of radiation reaching a plane object from a

small, circular, spatially incoherent source is measured. The data are in good agreement with the calculations made using the van Cittert-Zernike Theorem.

Motion of the object during the hologram exposure is shown to affect a quantity analogous to coherence. Such a quantity is introduced and it is shown that it affects the reconstruction in a way that is almost identical to that of partial coherence. The technique for measuring coherence is then extended to the measurement of displacements of the object. In particular, the relationship between the object displacement and the appearance of the reconstructed image is analyzed in detail for objects moving with constant or sinusoidal velocity. Several examples are given of measurements of the total displacement of objects moving with constant velocity throughout the exposure time. Displacements of one-third wavelength are easily detected.

APPROVAL OF DISSERTATION

EFFECTS OF PARTIAL COHERENCE ON HOLOGRAPHY

BY

MICHAEL LURIE

FOR

DEPARTMENT OF ELECTRICAL ENGINEERING

NEWARK COLLEGE OF ENGINEERING

BY

FACULTY COMMITTEE

APPROVED: _____ Chairman

_____

_____

NEWARK, NEW JERSEY

MAY, 1967

PREFACE

This dissertation concerns the process of electromagnetic wavefront reconstruction by holography, in particular the question of how the process is affected by the coherence of the electromagnetic radiation used.

The problem is approached in the following manner. First, a theoretical analysis of holography is performed, making only a few simplifying assumptions about the coherence (i.e. the statistics) of the electromagnetic radiation used to produce the hologram. Then some predictions of the analysis are confirmed experimentally. Finally, several applications of the findings are demonstrated.

The dissertation is organized in four parts.

Chapters 1 and 2 provide background material on holography and coherence at an introductory level. Some derivations are new, but these chapters are meant mainly as a review. A reader familiar with the subjects, or willing to accept the results, could omit these chapters. Appendices I and II are alternate descriptions of the hologram process. They are original, and as of this date have

not been published elsewhere. Appendix I discusses holography as a modulation process and may be of interest to readers with mainly electrical engineering backgrounds.

Chapter 3 begins the discussion of the research conducted for this dissertation. In that chapter we develop a theory of two-beam Fresnel and Fourier transform holography using partially coherent light, and analyze some properties of various images that can be reconstructed by these holograms. Chapter 3 contains nearly all the original theoretical development of the subject and provides the basis for the following chapters.

Chapters 4 and 5 demonstrate applications of the preceding theory, and in so doing, also confirm its validity. Considerable space is given to details of the experimental techniques and descriptions of the equipment used. Chapter 4 introduces the use of holography to measure spatial coherence and shows an example of such a measurement. Chapter 5 describes how holography can detect and measure small displacements. Holography of objects executing linear and sinusoidal motion are cited as examples and a measurement of linear motion is demonstrated.

Finally, Chapter 6 states some conclusions and recommendations for future work.

ACKNOWLEDGMENTS

I would like to thank Prof. Mauro Zambuto for suggesting this research and for encouraging my interest in optics. His advice and assistance have contributed a great deal to this dissertation. Our association has been a significant part of my education.

I am grateful to Newark College of Engineering for a one year fellowship that allowed me to devote my full attention to research.

Finally, I am especially indebted to my wife for her understanding and assistance. Without them this work could not have been completed or even begun.

TABLE OF CONTENTS

CHAPTER PAGE

I BASIC PRINCIPLES OF HOLOGRAPHY ---------- 1

1.1. Description of Holography and Properties of Holograms ------ 1

1.2. History of Holography ---------- 8

1.2.1. Single beam holograms (after Gabor) ----- 8

1.2.2. Two-beam holograms (after Leith and Upatnieks) -------- 11

1.3. Basic Theory of Holography with Coherent Illumination ---------- 12

II BASIC PRINCIPLES OF SECOND-ORDER COHERENCE ------- 21

2.1. Definition of Coherence as a Correlation Function ---- 21

2.2. Interference of Two Sources; an Example of a Coherence Effect ----- 25

2.3. Coherence at a Distance from an Extended Spatially Incoherent Source; the van Cittert-Zernike Theorem ---- 31

III A GENERALIZATION OF THE HOLOGRAM PROCESS TO PARTIALLY COHERENT, QUASI-MONOCHROMATIC, DIFFUSE ILLUMINATION ------ 36

3.1. Effects of Partial Coherence on Holography with Diffuse Illumination and a Plane Wave Reference Beam -- 36

3.2. Fourier Transform Holograms with Partially Coherent Light, a Special Case -- 48

3.2.1. The virtual images reconstructed by a Fourier transform hologram -- 48

3.2.2. Reconstruction of a real image from a Fourier transform hologram -- 60

IV HOLOGRAPHIC MEASUREMENT OF SPATIAL COHERENCE ----- 66

4.1. Production of Quasi-monochromatic Light with Known Spatial Coherence ----- 66

4.2. Description of Apparatus for Producing a Hologram of an Object Illuminated with Partially Coherent Light ---- 73

4.3. Measurement of Spatial Coherence by Means of a Hologram --- 82

V APPLICATION OF HOLOGRAPHY TO THE MEASUREMENT OF VERY SMALL MOTIONS ----- 90

5.1. Analysis of the Coherence of Radiation Reflected from a Moving Object ------ 90

5.2. Holographic Measurement of the Displacement of an Object Moving with Approximately Constant Velocity - 100

5.3. Additional Remarks on Holography of Moving Objects; Measurement of Sinusoidal Motion - 113

VI CONCLUSIONS AND RECOMMENDATIONS ---------- 117

APPENDIX

I AN EXPLANATION OF HOLOGRAPHY AS A MODULATION PROCESS ---- 122

II A PHYSICAL EXPLANATION OF HOLOGRAM RECONSTRUCTION ---------- 131

LIST OF FIGURES

FIGURE	PAGE
1-1	3
1-2	4
1-3a,b	6
1-3c	7
1-4	10
1-5	15
2-1	26
2-2	33
3-1	37
3-2	46
3-3	49
3-4	57
3-5	62
4-1	68
4-2	71
4-3	72
4-4	75
4-5	77
4-6	79
4-7	81
4-8a,b	84

FIGURE	PAGE
4-9	88
5-1	92
5-2	96
5-3	102
5-4	105
5-5	108
5-6	111
AI-1	123
AI-2	124
AI-3	126
AI-4	128
AII-1	133
AII-2	135
AII-3	137

LIST OF TABLES

TABLE	PAGE
4-1	87
5-1	112

CHAPTER I

BASIC PRINCIPLES OF HOLOGRAPHY

1.1. Description of Holography and Properties of Holograms

Holography is a process of recording all pertinent information about an electromagnetic wavefront and reconstructing it from the record. The hologram itself is such a record, usually a photograph, in the form of an interference pattern produced by radiation from a given source mixed with some standard, or reference, radiation. This interference pattern, which can be formed without the use of lenses, contains, in coded form, information about the amplitude and phase of the radiation at some surface, often a photographic plate. Thus, the hologram can be used to reconstruct the wavefront and, therefore, the original wave, by a suitable decoding process.

If the source is an object reflecting or transmitting light, then the hologram is, in very simple terms, a "picture" of that object, hence the popular name "lensless photography" for holography. However, there is little similarity between a hologram and a conventional

"snapshot." Viewing a hologram with ordinary light, such as is generated by an incandescent lamp, is unrewarding since the encoding process renders the recorded information meaningless to our eyes.

Figure 1-1 shows the appearance of a typical hologram, this one of an elephant silhouette viewed through a ring sight. (For a reconstructed image produced by this hologram, see Fig. 1-3a,b,c.) The original hologram is a black and white transparency; the figure is a print of it. By means of the appropriate decoding process which we will discuss later, this hologram can reproduce not just a picture of the object, but a duplicate of the actual radiation pattern that emanated from the object when the hologram was made.

One of many systems that can be used to produce a hologram is shown in Fig. 1-2. The light source would generally be a laser. A portion of the light is scattered by the object, while a different portion is specularly reflected by the mirror, directing a plane wave to the hologram plane. In this plane, interference between the plane wave reference beam reflected by the mirror and the light scattered by the object produces the hologram

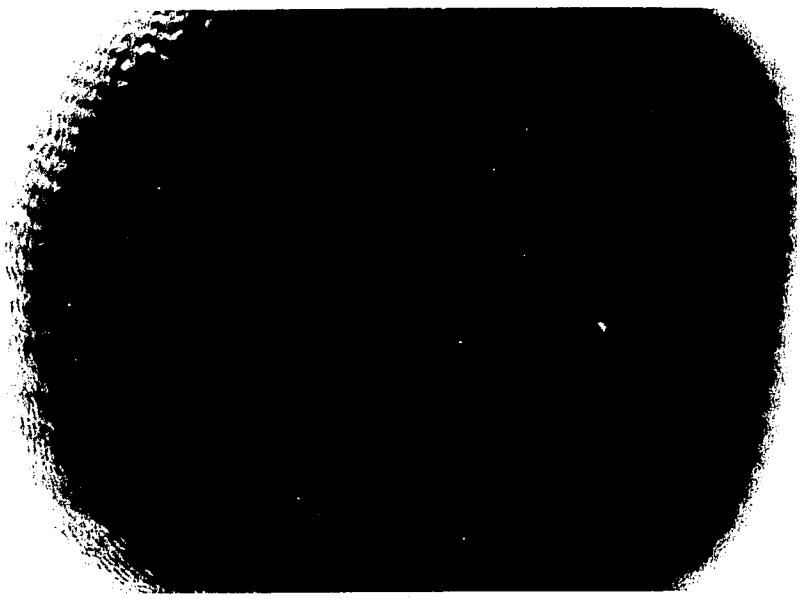

Figure 1-1. A typical hologram.

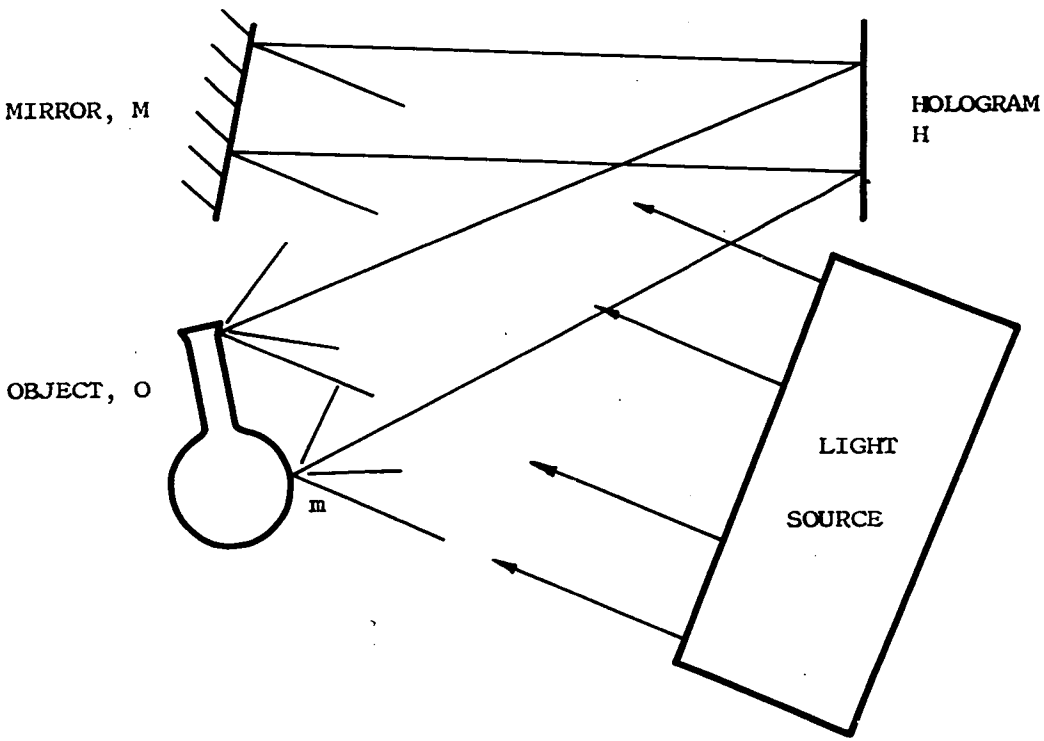

Figure 1-2. Apparatus for producing a hologram of a reflecting object O. A photographic plate in the plane H records the hologram.

which is generally recorded on a photographic emulsion. If a suitable wave is later passed through the processed photograph, a wavefront is reconstructed, part of which is identical to the wavefront originally produced by the object. According to Huygen's principle, this ultimately produces a virtual image identical to the object itself.

Before we investigate this system further, let us discuss some of the special properties of the holograms themselves.

An optical instrument such as the eye, a camera or a telescope, responds to the wavefront incident upon it. Since a portion of the holographically reconstructed wavefront is identical to the original wavefront from the object, an optical instrument cannot distinguish between them. If the object is three-dimensional, or is made up of several objects in different planes, then the reconstruction appears three-dimensional. Furthermore, this is a true three-dimensionality, not the artificial effect produced by stereoscopic pictures. An observer viewing a hologram reconstruction must refocus his eyes (or whatever instrument he is using) for near and distant objects, and also notices parallax. Figures 1-3a,b,c

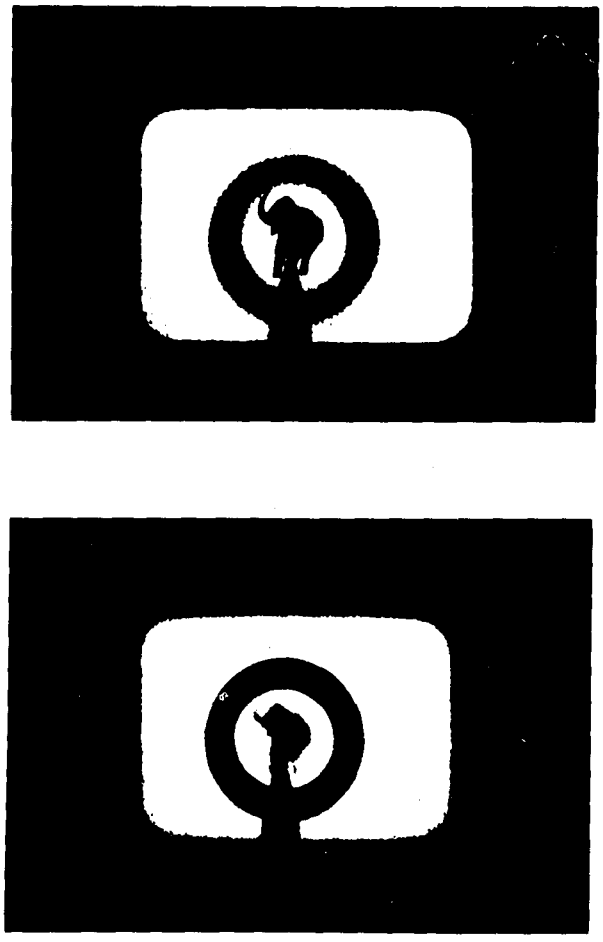

(a)

(b)

Figure 1-3. (a) A photograph, taken with a conventional 35mm camera, of a virtual image reconstructed by a hologram. The original subject was a slide of an elephant silhouette placed 1.25" behind a ring sight. The camera lens was set at f/2.8 and focussed on the elephant silhouette.

(b) A photograph of the same reconstruction, but with the camera focussed on the ring sight.

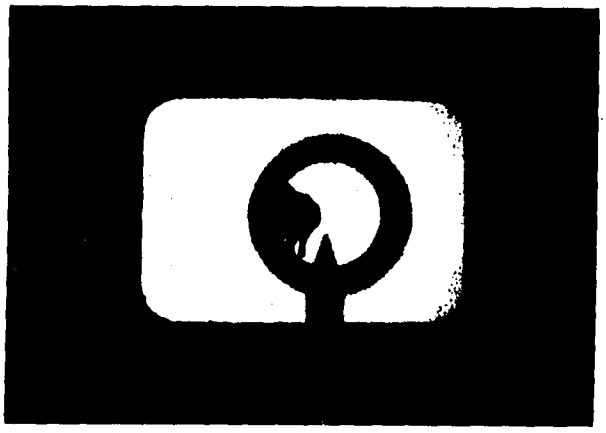

(c)

Figure 1-3. (c) A photograph of the same reconstruction, but with the camera moved to the left to demonstrate parallax in the image. Here, the camera lens was set to f/5.6 so that the entire subject could be in reasonably good focus.

are attempts to illustrate these properties within the limitations of conventional two-dimensional photographs. All these figures are photographs, made with an ordinary 35mm camera, of the image reconstructed with the hologram in Fig. 1-1. In Figs. 1-3a and b, the camera was focussed first on the elephant silhouette then on the ring, with the camera lens set at f/2.8 to give a small depth of field. It is apparent that the reconstructed image has depth; the images of the elephant and ring are at two different distances from the camera. Figure 1-3c was taken with the camera lens at f/5.6 so that both images could be in reasonably good focus. For Figs. 1-3a and b the camera was in line with the elephant and ring; for Fig. 1-3c it was moved to the left to demonstrate parallax.

1.2. History of Holography

1.2.1. Single beam holograms (after Gabor). The concept of holography was first proposed by Gabor [1,2] in 1948 as a technique for producing images in electron microscopes without using lenses, thereby eliminating the large distortion of electron lenses. Many practical problems were encountered, particularly the lack of

coherent electron beams needed to produce good interference patterns; even recent attempts at holographic electron microscopy by Kirkpatrick and El-Sum[3] have not been encouraging.

Gabor's process had serious drawbacks even when visible light was used instead of electron beams. First, in 1948, highly coherent light could be produced only with great difficulty and at very low power levels. Second, and of more fundamental importance, holograms generally produce two images of the original object as a consequence of the encoding and decoding processes as we will show later in Section 1.3. In Gabor's holograms both images lie on one axis so that one is viewed superimposed on the other. This blurred "ghost" image destroys the clarity and sharpness of the desired image.

Gabor's procedure remains the simplest way to produce a hologram. He simply placed an object such as a slide so as to partially obscure a coherent beam, then recorded the interference pattern resulting from the unobscured portion of the beam and the portion diffracted by the object, as shown in Fig. 1-4. In spite of the simplicity, this method is no longer used for several

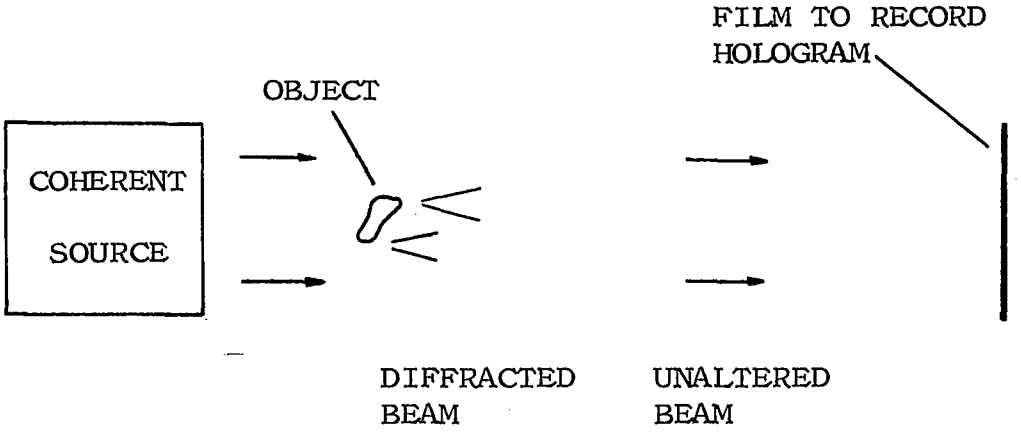

Figure 1-4. Producing a hologram by Gabor's single beam method.

reasons: the ghost images mentioned previously, the poor results with objects having large opaque areas, and the extreme sensitivity of the holograms to common photographic imperfections such as dust and scratches.

1.2.2. Two-beam holograms (after Leith and Upatnieks). A significant advance in holography was reported in 1962 by E. Leith and J. Upatnieks[4]. They described a variation on Gabor's technique that produced the two reconstructed images on different axes, that is, not one behind the other, so that two high quality images were formed that could be viewed separately. Furthermore, by 1962 lasers could provide light that was more intense and more highly coherent than that previously available.

Leith and Upatnieks used separate beams, one for a reference beam and another to illuminate the object. Although the beams are from the same source, they can be individually aimed and adjusted in intensity. This freedom permits the positioning of the two reconstructions on different axes. The hologram system shown schematically in Fig. 1-2 is of the two-beam type.

Nearly all modern holograms are made with this simple system, frequently with some not so simple variations. The next section discusses the basic theory of two-beam holograms and reconstructions.

For the remainder of this paper, the word "hologram" will refer to the two-beam type unless specified otherwise.

1.3. Basic Theory of Holography with Coherent Illumination

Of the many ways to describe the theory of holography, the most straightforward seems to be simply to write out the distribution of energy acting on the photographic plate or film that will be the hologram and, from this, to calculate the wavefront produced when a beam passes through the developed plate in the reconstruction process. This reconstructed wavefront should contain a portion identical to the original wavefront produced by the object itself. Two alternate descriptions by the author appear in the Appendices. Appendix I discusses holography from the modulation point of view, while Appendix II provides a more physical approach.

Referring[5] back to Fig. 1-2, let

$$a(P)\cos\left[\omega t+\alpha(P)\right]$$

represent analytically an appropriate characteristic of the electromagnetic field at the hologram plane H due to the radiation from the illuminated object only. Similarly, let

$$b\cos\left[\omega t+\beta(P)\right]$$

represent the same characteristic of the electromagnetic field at H due to the reference beam only. Such expressions are generally referred to as analytic signals. The characteristic represented can be one of several, e.g. electric field, magnetic field, vector potential, etc., each of which has three components that are completely determined by their amplitudes and phases. For simplicity, we may assume here that all the radiation considered is polarized in nearly the same direction so that only one component of any characteristic of the field must be considered. This is generally done in optics problems, although the justification is extremely difficult[6].

The above analytic representations are functions of time and of the point P in the hologram plane H. The amplitude b of the reference electromagnetic field at H is assumed to be constant over the hologram surface. The total electromagnetic field at H can be represented by

$$F(P,t) = a(P)\cos[\omega t + \alpha(P)] + b\cos[\omega t + \beta(P)] \quad . \qquad (1\text{-}1)$$

However, a photographic emulsion does not respond to the incident amplitude. We will assume here, again for simplicity, that the plate responds linearly to energy, that is, that after proper processing, the amplitude transmittance of the photograph exposed at the plane H for a time T can be made to be

$$A(P,T) = K\int_0^T |F(P,t)|^2\, dt$$

where K is a proportionality constant. Evaluating this integral using Eqn. 1-1 shows that each of the terms in A(P,t) contains either T or $1/\omega$. Since $T \gg 1/\omega$, only those terms containing T are significant. Then, to an excellent approximation,

$$A(P,T) = \tfrac{1}{2} KT\left[a^2(P) + b^2 + 2a(P)b\cos[\alpha(P) - \beta(P)]\right] .$$

The photograph with this amplitude transmittance is a hologram, and we will now show that with it we can reconstruct the original wave from the object.

If radiation of frequency ω is incident on the hologram as in Fig. 1-5 and generates there a wavefront

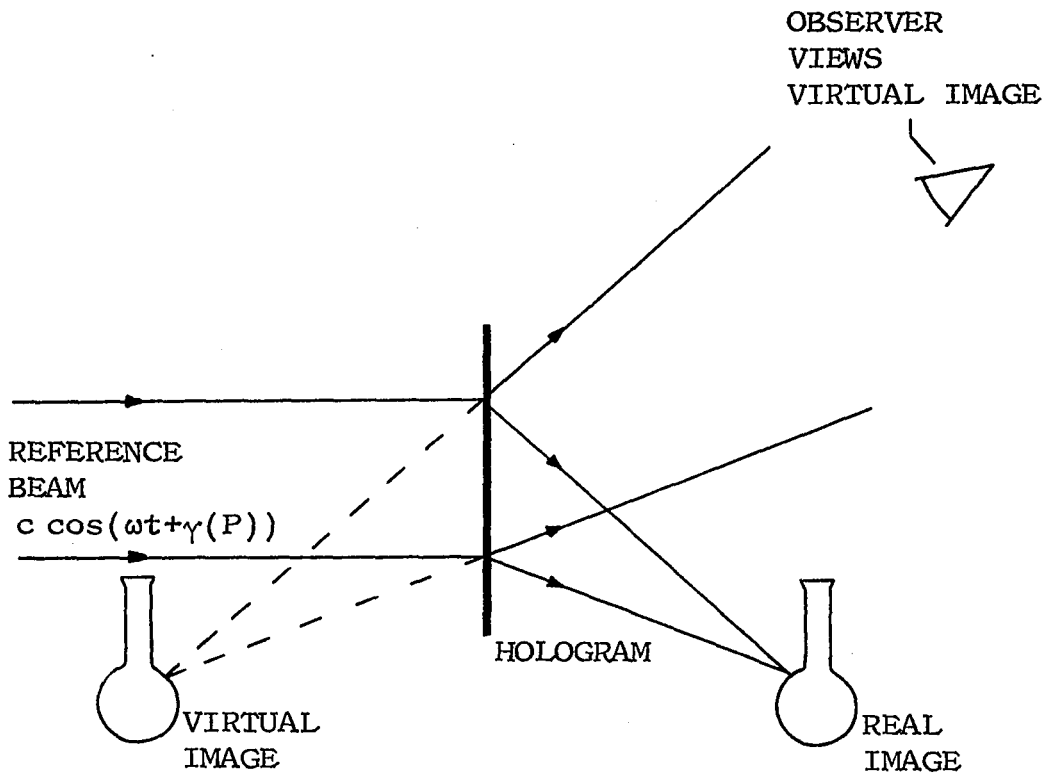

Figure 1-5. Reconstructing a hologram.

$$c \cos[\omega t + \gamma(P)]$$

of constant amplitude c over the surface of the hologram, then the transmitted wavefront is

$$A(P,t)c\cos[\omega t+\gamma(P)] = \tfrac{1}{2}cKT\left[a^2(P)+b^2\right]\cos[\omega t+\gamma(P)]$$

$$+ bcKTa(P)\cos[\alpha(P)-\beta(P)]\cos[\omega t+\gamma(P)] .$$

The first term in the sum represents some wavefront that is of little interest because it does not result in a recognizable image, but the second term we want to study further. Expanding the product of the cosines, we can write this term as $U(P,t)_+ + U(P,t)_-$ where

$$U(P,t)_{\pm} = \left[\tfrac{1}{2}bcKT\right]a(P)\cos[\omega t \pm \alpha(P) \mp \beta(P) + \gamma(P)] . \qquad (1-2)$$

If the reconstructing beam is of the same form as the reference beam, then

$$\gamma(P) = \beta(P)$$

and

$$U(P,t)_+ = \left[\tfrac{1}{2}bcKT\right]a(P)\cos[\omega t + \alpha(P)]$$

which is the same as the original wave from the object, aside from the unimportant constant amplitude factor in the first square bracket. Therefore, when the observer indicated in Fig. 1-5 looks through the hologram, he sees

a virtual image identical to the object.

If instead we make $\gamma(P) = -\beta(P)$, the term $U(P,t)_-$ differs from the term $U(P,t)_+$ above only in having opposite phase, $-\alpha(P)$. Whereas the wavefront $U(P,t)_+$ appears to diverge from a virtual image, the wavefront $U(P,t)_-$ may be shown to converge to form a real image, generally called the conjugate image. This conjugate image can be projected on a screen or film. In the latter instance the film will produce a photograph of the object. Recalling that no lenses were used either to produce the hologram or the reconstruction, we see more clearly than before the origin of the popular term "lensless photography" for holography.

At this point it may be instructive to consider one particularly simple form of reference beam and reconstruction beam in detail. If a hologram is made with a normally incident plane wave reference beam of constant amplitude, then the wavefronts are parallel to the hologram surface, and the reference beam at that surface is simply

$$b\cos\omega t \quad .$$

Clearly, for this case, $\beta(P) = 0$ for all P. Let us

position the object to one side of the normal to the hologram, as indicated in Fig. 1-2. As above, the radiation at the point P of the hologram, from the object, is written as

$$a(P)\cos\left[\omega t+\alpha(P)\right] .$$

If the resulting hologram is reconstructed with a normally incident plane wave, then $\gamma(P) = 0$ and we find from the calculations above, particularly Eqn. 1-2, that

$$U(P,t)_{+} = \left[\tfrac{1}{2} bcKT\right] a(P) \cos\left[\omega t + \alpha(P)\right]$$

and

$$U(P,t)_{-} = \left[\tfrac{1}{2} bcKT\right] a(P) \cos\left[\omega t - \alpha(P)\right] .$$

Obviously $U(P,t)_{+}$ is an exact reproduction of the wave from the object with only a change in amplitude, and produces the virtual image shown in Fig. 1-5, while $U(P,t)_{-}$ differs from $U(P,t)_{+}$ by the sign of $\alpha(P)$. The phase distribution $\alpha(P)$ over the hologram surface represents waves that are diverging from the object which is located away from the normal to the hologram, that is, waves that are concave towards the object and inclined with respect to the hologram surface. $-\alpha(P)$ represents waves of the same curvature but concave away from the object and of opposite inclination, hence producing

converging rays and the real image shown in Fig. 1-5. Note particularly that the two images lie on different axes; the real image is away from the line of sight when an observer looks through the hologram to see the virtual image, and the diverging rays from the virtual image will not fall on a screen placed to display the real image [7].

The preceding discussion, while explaining the hologram process accurately, implies an assumption so fundamental that it is easily overlooked. In writing the various waves as simple sinusoids we have precluded the possibility of statistical variations among them. The relationship between the phases of the reference and object beams is known precisely at all points for all time. This is equivalent to complete coherence. We will remove this restriction in Chapter 3 after developing techniques for handling the statistics of electromagnetic fields in Chapter 2.

REFERENCES

1. D. Gabor, Nature 161, 777 (1948).

2. D. Gabor, Nature 162, 764 (1948).

3. P. Kirkpatrick and H. M. A. El-Sum, J.Opt.Soc.Am.46, 825 (1956).

4. E. Leith and J. Upatnieks, J.Opt.Soc.Am.52, 1123 (1962).

5. This explanation was first suggested by Dr. Mauro Zambuto, private communication.

6. M. Beran and G. Parrent, Theory of Partial Coherence, Prentice Hall, N. J., 1964, p. 27.

7. For a very detailed and general discussion of holographic reconstruction from a similar point of view, the reader is referred to:
R. W. Meier, J.Opt.Soc.Am.55, 987 (1965).

CHAPTER II

BASIC PRINCIPLES OF SECOND-ORDER COHERENCE

2.1. Definition of Coherence as a Correlation Function

An important property of radiation is its degree of coherence, described in terms of the correlation between the analytic signal (see Chapter 1) at some point and time and the analytic signal at some other point and some other time. In particular, we somewhat artificially distinguish between two aspects of coherence, although they are interrelated:

> Spatial coherence - the correlation between the analytic signals measured at different points, at the same time,

and

> Temporal coherence - the correlation between the analytic signals measured at different times, but at the same point.

Notice that a wave containing only one frequency, in optics a monochromatic wave, must be coherent and a non-monochromatic wave cannot be completely coherent. We will generally consider quasi-monochromatic (narrow bandwidth) waves in this paper. For efficiency, quasi-

monochromatic will be abbreviated as q-m from now on.

The coherence effects described above are called second-order coherence effects because they involve the correlation of the analytic signals at two space-time points[1]. We will now introduce precise definitions of second-order coherence.

Let $V(P_1,t+\tau)$ and $V(P_2,t)$ be the analytic signals representing two waves, or portions of the same wave, measured at the points P_1 and P_2 at time intervals spaced τ apart. The analytic signal $V(P,t)$ is a scalar, proportional to the complex amplitude (amplitude and phase) of the appropriate electromagnetic field vector. As was pointed out in Chapter 1, a scalar can be used to represent the field if all the radiation is polarized in one direction. Then, in free space or air, the direction of the field is always known and $V(P,t)$, which tells the magnitude and phase of the field as a function of position and time, completely describes the field.

If we define a quantity $I(P)$ to be proportional to the power per unit area of the radiation at P, then

$$\langle I(P_i)\rangle = \langle V(P_i,t)V^*(P_i,t)\rangle$$

and

$$\langle I(P_2)\rangle = \langle V(P_2,t)V^*(P_2,t)\rangle$$

where * denotes a complex conjugate and the pointed brackets denote a time average. The quantity $\langle I(P)\rangle$ has more physical significance that I(P) since, at optical frequencies ($\sim 10^{14}$Hz), only time averages can be measured. We can also define

$$\Gamma_{12}(\tau) = \langle V(P_1,t+\tau)V^*(P_2,t)\rangle \qquad (2\text{-}1)$$

where the subscripts on Γ refer to P_1 and P_2. $\Gamma_{12}(\tau)$ is called the mutual coherence function and represents the correlation between the wave at P_2 and the wave at P_1 considered at a time τ later[2]. $\Gamma_{12}(\tau)$ is clearly a cross-correlation[3] since, from the definition of the pointed brackets,

$$\Gamma_{12}(\tau) = \lim_{T\to\infty}\frac{1}{2T}\int_{-T}^{T} V(P_1,t+\tau)V^*(P_2,t)\,dt \quad .$$

From the definition of Γ in Eqn. 2-1, $\Gamma_{11}(\tau)$ is a measure of what we called temporal coherence at the point 1, as defined at the beginning of this chapter. Likewise, $\Gamma_{12}(0)$ measures the spatial coherence at the points 1 and 2. Notice that

$$\Gamma_{11}(0) = \langle V(P_1,t)V^*(P_1,t)\rangle = \langle I(P_1)\rangle \qquad (2\text{-}2)$$

It will be convenient to normalize Γ for later use.

Let

$$\gamma_{12}(\tau) = \frac{\Gamma_{12}(\tau)}{\sqrt{\Gamma_{11}(0)\,\Gamma_{22}(0)}}$$

$$= \frac{\lim_{T\to\infty} \frac{1}{2T} \int_{-T}^{T} V(P_1, t+\tau) V^*(P_2, t)\, dt}{\sqrt{\langle I(P_1)\rangle \langle I(P_2)\rangle}} \quad . \qquad (2\text{-}3)$$

It can be shown[4] by means of the Schwarz inequality that

$$0 \leq |\gamma_{12}(\tau)| \leq 1 \quad .$$

$\gamma_{12}(\tau)$ is called the complex degree of coherence. For completely coherent radiation, $|\gamma_{12}(\tau)| = 1$; for incoherent radiation, $|\gamma_{12}(\tau)| = 0$; for partially coherent radiation $|\gamma_{12}(\tau)|$ can have any value between these.

One special situation is noteworthy. If the radiation occupies only a narrow band of frequencies $\Delta\omega$ about ω such that

$$\Delta\omega \ll 1/\tau \qquad (2\text{-}4)$$

for all τ of interest, then we can approximate[5]

$$\gamma_{12}(\tau) \approx \gamma_{12}(0)\, e^{-j\omega\tau} \quad . \qquad (2\text{-}5)$$

We can now define q-m (quasi-monochromatic) light more precisely than at the beginning of this chapter:

> q-m light obeys the narrow-band approximation 2-4 above.

Note that τ is not a property of the light, but a condition imposed by a particular experiment or calculation, so a beam that may be considered q-m in one situation may not be in another involving a longer τ. Finally, it is clear that the terms q-m and temporally coherent are equivalent since, for q-m light,

$$|\gamma_{11}(\tau)| = |\gamma_{11}(0)\, e^{-j\omega\tau}| = 1 .$$

2.2. Interference of Two Sources; an Example of a Coherence Effect

Consider the interference pattern formed on a screen by radiation coming from two point sources at P_1 and P_2 as in Fig. 2-1. We will specifically not assume that the two sources have a constant phase relationship as is done in elementary electromagnetic theory texts.

Let $V(P_1,t)$ be the analytic signal that describes the electric field produced at P_1 at time t, and define $V(P_2,t)$ similarly. For a point Q on a screen at distances s_1 and s_2 from P_1 and P_2 respectively, we can write

$$V(Q,t) = \frac{1}{q(s_1)} V\left(P_1, t - \frac{s_1}{c}\right) + \frac{1}{q'(s_2)} V\left(P_2, t - \frac{s_2}{c}\right)$$

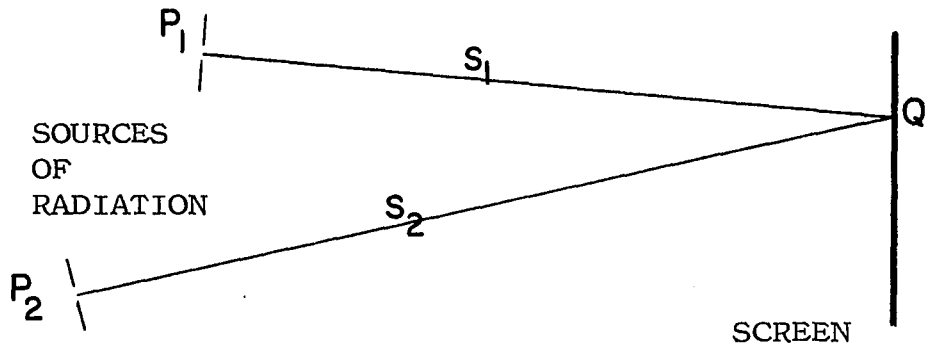

Figure 2-1. Interference of two sources, P_1 and P_2.

where $1/g(s_1)$ and $1/g'(s_2)$ are dimensionless ratios* and c is the speed of light.

The time average irradiance[6] (power per unit area) at a point Q is given by

$$\begin{aligned}\langle I(Q)\rangle &= \langle V(Q,t)V^*(Q,t)\rangle \\ &= \frac{1}{g(s_1)^2}\left\langle V(P_1, t-\tfrac{s_1}{c})V^*(P_1, t-\tfrac{s_1}{c})\right\rangle \\ &\quad + \frac{1}{g'(s_2)^2}\left\langle V(P_2, t-\tfrac{s_2}{c})V^*(P_2, t-\tfrac{s_2}{c})\right\rangle \\ &\quad + \frac{2}{g(s_1)g'(s_2)}\,\mathrm{Re}\left\langle V(P_1, t-\tfrac{s_1}{c})V^*(P_2, t-\tfrac{s_2}{c})\right\rangle .\end{aligned} \tag{2-6}$$

Let us examine the last equation term by term. For

---

*The functions g(s) and g'(s) depend on the type of propagation of the radiation. For instance, for a plane wave, g(s) = 1, whereas for a hemispherical wave coming from a hemispherical radiator of radius ρ,

$$g(s) = \sqrt{2\pi\rho^2/2\pi s^2} = \rho/s$$

since in that case

$$V(Q,t) = \sqrt{2\pi\rho^2/2\pi s^2}\; V(P, t-\tfrac{s-\rho}{c})$$

and, if the radius ρ of the source is much less than s

$$V(Q,t) \approx \sqrt{2\pi\rho^2/2\pi s^2}\; V(P, t-\tfrac{s}{c}) .$$

For a more general type of wave, g(s) could be quite complicated. The major effect of g(s) is a relative variation of the amplitude of the analytic signal at different positions with respect to the source. In all cases of interest here, the geometry is such that these variations are negligible. Nevertheless, we carry the functions through our calculations.

stationary statistics, the time averages are independent of the choice of the time origin, so

$$\langle V(P_1, t-\tfrac{s_1}{c})\, V^*(P_1, t-\tfrac{s_1}{c})\rangle = \langle V(P_1,t)V^*(P_1,t)\rangle = \langle I(P_1)\rangle$$

and

$$\langle V(P_2, t-\tfrac{s_2}{c})\, V^*(P_2, t-\tfrac{s_2}{c})\rangle = \langle I(P_2)\rangle \ .$$

By the same argument,

$$\langle V(P_1, t-\tfrac{s_1}{c})\, V^*(P_2, t-\tfrac{s_2}{c})\rangle$$

$$= \langle V(P_1, t+\tau)\, V^*(P_2, t)\rangle = \Gamma_{12}(\tau)$$

where $\tau = \dfrac{s_2 - s_1}{c}$.

Now Eqn. 2-6 can be rewritten as

$$\langle I(Q)\rangle = \frac{1}{g(s_1)^2}\langle I(P_1)\rangle + \frac{1}{g'(s_2)^2}\langle I(P_2)\rangle + \frac{2}{g(s_1)g'(s_2)}\,\mathrm{Re}\,\Gamma_{12}(\tau) .$$

If the source at P_1 were removed, then $\langle I(Q)\rangle$ due to the source at P_2 only would be

$$\langle I^{(2)}(Q)\rangle = \frac{1}{g'(s_2)^2}\langle I(P_2)\rangle \ .$$

Similarly, define

$$\langle I^{(1)}(Q)\rangle = \frac{1}{g(s_1)^2}\langle I(P_1)\rangle \ .$$

Furthermore,

$$\Gamma_{12}(\tau) = \gamma_{12}(\tau)\sqrt{\langle I(P_1)\rangle\langle I(P_2)\rangle}$$

so

$$\frac{2}{g(s_1)g'(s_2)}\,\mathrm{Re}\,\Gamma_{12}(\tau) = 2\sqrt{\langle I^{(1)}(Q)\rangle\langle I^{(2)}(Q)\rangle}\,\mathrm{Re}\,\gamma_{12}(\tau).$$

These substitutions yield

$$\langle I(Q)\rangle = \langle I^{(1)}(Q)\rangle + \langle I^{(2)}(Q)\rangle + 2\sqrt{\langle I^{(1)}(Q)\rangle\langle I^{(2)}(Q)\rangle}\ \mathrm{Re}\,\gamma_{12}(\tau) .$$

To reveal the significance of this result, write

$$\gamma_{12}(\tau) = |\gamma_{12}(\tau)|\, e^{j\alpha(\tau)} \qquad (2\text{-}7)$$

where

$$\alpha(\tau) = \arg \gamma_{12}(\tau) .$$

Then

$$\mathrm{Re}\,\gamma_{12}(\tau) = |\gamma_{12}(\tau)| \cos\alpha(\tau)$$

and we can write the equation for the interference of two point sources as

$$\langle I(Q)\rangle = \langle I^{(1)}(Q)\rangle + \langle I^{(2)}(Q)\rangle + 2\sqrt{\langle I^{(1)}(Q)\rangle\langle I^{(2)}(Q)\rangle}\ |\gamma_{12}(\tau)| \cos\alpha(\tau) . \qquad (2\text{-}8)$$

$\alpha(\tau) = \alpha(\frac{s_2 - s_1}{c})$ and depends on s_2 and s_1, i.e. $\alpha(\tau)$ varies with Q, the position on the screen. As various Q's are considered, $\cos\alpha(\tau)$ varies from 1 to -1.

We can define the visibility (or contrast) of the interference pattern as

$$\mathcal{V} = \frac{\langle I(Q)\rangle_{max} - \langle I(Q)\rangle_{min}}{\langle I(Q)\rangle_{max} + \langle I(Q)\rangle_{min}} .$$

Here

$$\langle I(Q)\rangle_{max} = \langle I^{(1)}(Q)\rangle + \langle I^{(2)}(Q)\rangle + 2\sqrt{\langle I^{(1)}(Q)\rangle\langle I^{(2)}(Q)\rangle}\,\left|\gamma_{12}(\tau)\right|$$

and

$$\langle I(Q)\rangle_{min} = \langle I^{(1)}(Q)\rangle + \langle I^{(2)}(Q)\rangle - 2\sqrt{\langle I^{(1)}(Q)\rangle\langle I^{(2)}(Q)\rangle}\,\left|\gamma_{12}(\tau)\right|$$

so that

$$\mathcal{V} = \frac{2\sqrt{\langle I^{(1)}(Q)\rangle\langle I^{(2)}(Q)\rangle}}{\langle I^{(1)}(Q)\rangle + \langle I^{(2)}(Q)\rangle}\,\left|\gamma_{12}(\tau)\right| .$$

Clearly, $\mathcal{V}$ is proportional to $\left|\gamma_{12}(\tau)\right|$.

For the special case of equal intensity of the two sources,

$$\langle I^{(1)}(Q)\rangle = \langle I^{(2)}(Q)\rangle$$

and we have the particularly simple result

$$\mathcal{V} = \left|\gamma_{12}(\tau)\right| .$$

For incoherent light $\left|\gamma_{12}(\tau)\right| = 0$, and the pattern is not visible. For coherent light, $\left|\gamma_{12}(\tau)\right| = 1$, $\langle I(Q)\rangle_{min} = 0$, and we observe an interference pattern with true nulls at the minima.

This result is often used to measure the coherence of radiation at two points. The radiation from the two points is made to interfere, and the visibility of the resulting pattern is measured. This is difficult and

tedious, since the measurement must be repeated for every set of points of interest. In Chapter 4, a holographic technique is demonstrated by which the coherence of radiation over an entire surface can be measured with respect to one reference point. The development of this technique may be the major result of this work.

Although the interference pattern of which a hologram is made is formed by a large number of point sources, the above discussion of visibility does suggest that partially coherent light should produce a hologram that is degraded in some way, while incoherent light should produce no hologram at all. The precise way in which partial coherence affects the hologram will be analyzed in Chapter 3.

2.3. Coherence at a Distance from an Extended Spatially Incoherent Source; the van Cittert-Zernike Theorem

In designing experiments using partially coherent light (cf. Chapter 4), we will frequently use the van Cittert-Zernike Theorem. This permits the calculation of the mutual coherence at two points illuminated by a spatially incoherent (q-m) source whose dimensions are much smaller than the distance from the source to the points. The result is important in experiments with

partially coherent light because it provides a method for the production of a known coherence distribution $\Gamma_{12}(\tau)$ in space by the use of an appropriate incoherent source. Detailed derivations and discussions of this theorem can be found in the literature[1,7,8,9,10].

Referring to Fig. 2-2, if σ is a spatially incoherent (q-m) source having center frequency and wavelength ω and λ respectively, and intensity I(S) at each element of area dS, the theorem states that $\Gamma_{12}(\tau)$, the coherence at points P_1 and P_2 measured at times differing by τ is

$$\Gamma_{12}(\tau) \cong \frac{1}{\lambda^2} e^{-j\omega\tau} \int_{\sigma} \frac{I(S)}{r_1 r_2} e^{-j\omega\left(\frac{r_1 - r_2}{c}\right)} dS \quad . \qquad (2\text{-}9)$$

In particular, if we let σ be a uniform, circular source of radius ρ and let P_1 and P_2 lie in a plane parallel to this source, situated so that $\overline{P_1P_2}$, the distance between P_1 and P_2, is much less than R, the distance from the source to the plane of P_1 and P_2, the resulting normalized expression is

$$\gamma_{12}(\tau) = \left(\frac{2J_1(v)}{v} \right) e^{-j(\beta - \omega\tau)} \qquad (2\text{-}10)$$

where

$$\beta = \frac{\pi}{\lambda R} (r_2^2 - r_1^2) \quad ,$$

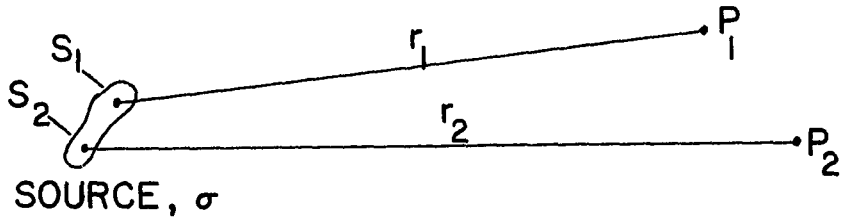

Figure 2-2. The geometry for calculating the coherence at P_1 and P_2 of radiation from an arbitrary source.

and $$v = \frac{2\pi}{\lambda}\left(\frac{\rho}{R}\right)\left(\overline{P_1 P_2}\right)$$

and J_1 is the Bessel function of the first kind, first order.

Note the particularly simple relation

$$\left|\gamma_{12}(\tau)\right| = \left|\frac{2J_1(v)}{v}\right| \quad . \qquad (2\text{-}11)$$

In the following chapters we will make use of the fact that, as shown by Eqn. 2-11, a small, circular, incoherent, q-m source can be used to illuminate a plane with light of known coherence.

REFERENCES

1. L. Mandel and E. Wolf, Rev.Mod.Phys.2, 231 (1965).
2. M. Born and E. Wolf, Principles of Optics, 2d. ed., Pergamon Press, N. Y., 1964, p. 500.
3. W. B. Davenport, Jr. and W. L. Root, An Introduction to the Theory of Random Signals and Noise, McGraw-Hill, Inc., N. Y., 1958, p.70.
4. M. Born and E. Wolf, op.cit., p.502.
5. Ibid., p.507.
6. The International Dictionary of Physics and Electronics, 2d. ed., D. Van Nostrand Co., Inc., N. J., 1961.
7. M. Born and E. Wolf, op.cit., p.508.
8. M. Beran and G. Parrent, Theory of Partial Coherence, Prentice Hall, N. J., 1964, p.13.
9. P. H. van Cittert, Physica 1, 201 (1934).
10. F. Zernike, Physica 5, 785 (1938).

CHAPTER III

A GENERALIZATION OF THE HOLOGRAM PROCESS TO PARTIALLY COHERENT, QUASI-MONOCHROMATIC, DIFFUSE ILLUMINATION

3.1. Effects of Partial Coherence on Holography with Diffuse Illumination and a Plane Wave Reference Beam[1]

The discussion of the hologram process in Chapter 1 had two significant limitations. First, by dealing only with the analytic signal at the hologram plane, discussion of the details of any phenomena occurring at the object was made impossible. Examples of such phenomena include motion of some point of the object and the coherence of the light at the object. Second, by writing the various analytic signals as simple sinusoidal functions, complete coherence was implicitly assumed. To remove these limitations, we will now analyze the hologram process in more detail.

Figure 3-1 shows a possible arrangement for producing a hologram of an object O. For simplicity, we assume an illuminated object and impose the following restrictions on the radiation leaving the object and the reference beam source:

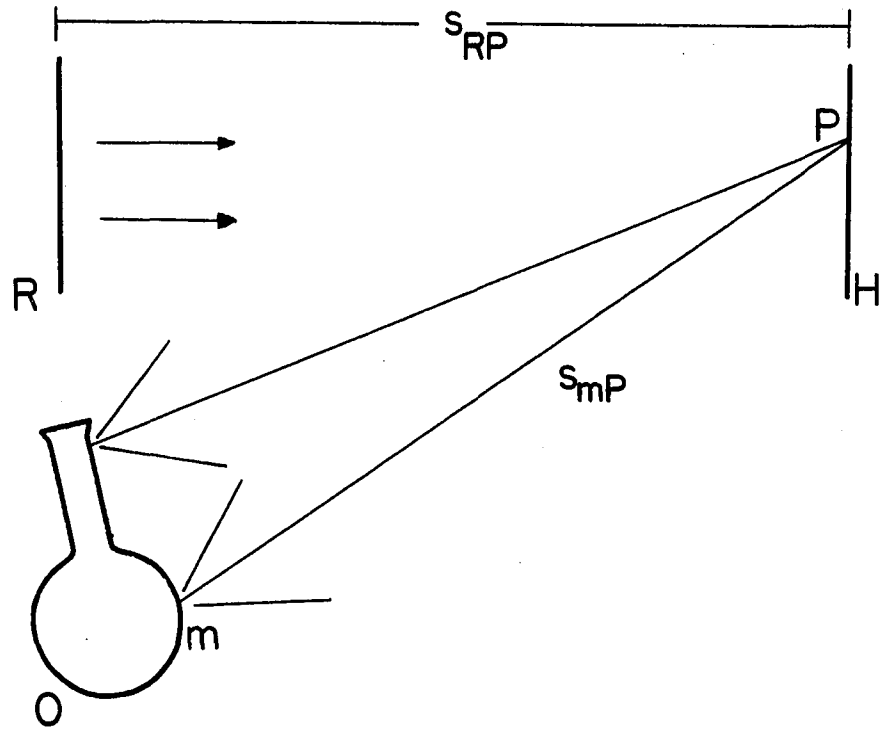

Figure 3-1. A system for producing a hologram in the plane H. P is any point in that plane. R is the source of the plane wave reference beam. O is an illuminated, diffusely reflecting object. s_{RP} and s_{mP} are the distances indicated.

a) All the radiation is q-m and polarized in nearly the same direction, as was discussed in Chapter 1.

b) The reference beam is a plane wave, spatially coherent and of uniform radiance.

A photographic plate in the plane H would record the integral over the exposure time of the irradiance at each point P in the plane. However, we generally speak in terms of the time average irradiance rather than the integral over time. If $V_P(t)$, the analytic signal at P, is a stationary random function of time, or a periodic function of time, then, for any given exposure time T sufficiently long compared to the duration of fluctuations in, or the period of $V_P(t)$, the integral over T of the irradiance at P is proportional to the time average irradiance $\langle I(P) \rangle$ given by

$$\langle I(P) \rangle = \langle V_P(t) V_P^*(t) \rangle \ ,$$

where the pointed brackets denote a time average and $V_P(t)$ is the analytic signal reaching the point P at time t. Consider the object O as made up of many small elements m and let $V_{mP}(t)$ be the analytic signal at P due to the radiation from the m^{th} element on O. Further, let $V_{RP}(t)$ be the analytic signal at P due to the plane wave reference beam. Then

$$V_P(t) = V_{RP}(t) + \sum_m V_{mP}(t) \quad .$$

It follows after some simplification, that

$$\langle I(P) \rangle = \sum_m \sum_n \langle V_{mP}(t) V_{nP}^*(t) \rangle \qquad (3-1)$$

$$+ \langle V_{RP}(t) V_{RP}^*(t) \rangle + \sum_m 2 \mathrm{Re} \langle V_{mP}(t) V_{RP}^*(t) \rangle$$

or

$$\langle I(P) \rangle = \langle I_o(P) \rangle + \langle I_R(P) \rangle + 2 \sum_m \mathrm{Re} \langle V_{RP}(t) V_{mP}^*(t) \rangle \qquad (3-2)$$

where $I_o(P)$ represents the first term in Eqn. 3-1 and is the irradiance at P due to all the radiation from O without the reference beam, and $I_R(P)$ represents the second term in Eqn. 3-1 and is the irradiance at P due to the reference beam only, and where

$$\mathrm{Re} \langle V_{mP}(t) V_{RP}^*(t) \rangle = \mathrm{Re} \langle V_{RP}(t) V_{mP}^*(t) \rangle \, .$$

For the special case of a plane wave reference beam of uniform amplitude, $I_R(P)$ is constant for all P. We will now show that the last term in Eqn. 3-2 can be expressed compactly in terms of the coherence between the radiation leaving the reference beam source and the radiation leaving the element m of the object.

Consider q-m radiation so ω is a good approximation to the entire bandwidth. If $V_R(t)$ and $V_m(t)$ are the

analytic signals at the reference beam source and at the element m of the object, respectively,

$$V_{RP}(t) = V_R(t-\frac{s_{RP}}{c})$$

and

$$V_{mP}(t) = \frac{1}{g(s_{mP})} V_m(t-\frac{s_{mP}}{c}) \quad ,$$

where, as in Chapter 2, $1/g(s_{mP})$ is a dimensionless ratio that shows how the amplitude of the analytic signal decreases with distance from the source. Therefore,

$$\begin{aligned} \mathrm{Re}\left\langle V_{RP}(t)V^*_{mP}(t)\right\rangle &= \mathrm{Re}\left\langle V_R(t-s_{RP}/c)V^*_m(t-s_{mP}/c)\right\rangle \frac{1}{g(s_{mP})} \\ &= \frac{1}{g(s_{mP})}\mathrm{Re}\left\langle V_R(t)V^*_m(t+\frac{s_{RP}-s_{mP}}{c})\right\rangle \quad . \end{aligned} \tag{3-3}$$

Letting $\tau_{mRP} = \frac{s_{mP}-s_{RP}}{c}$, we can write according to the definitions in Eqns. 2-1 and 2-3,

$$\begin{aligned} \gamma_{Rm}(\tau_{mRP}) &= \frac{\langle V_R(t+\tau_{mRP})V^*_m(t)\rangle}{\left[\langle V_R(t)V^*_R(t)\rangle\langle V_m(t)V^*_m(t)\rangle\right]^{\frac{1}{2}}} \\ &= \frac{\langle V_R(t)V^*_m(t-\tau_{mRP})\rangle}{\left[\langle V_R(t)V^*_R(t)\rangle\langle V_m(t)V^*_m(t)\rangle\right]^{\frac{1}{2}}} \quad . \end{aligned} \tag{3-4}$$

$\gamma_{Rm}(\tau_{mRP})$ is the complex degree of coherence between the radiation leaving any element m at time $(t-\tau_{mRP})$ and the radiation leaving the reference beam source at time t.

Let $\langle I(R)\rangle$ and $\langle I(m)\rangle$ be given by

$$\langle I(R)\rangle = \langle V_R(t)V^*_R(t)\rangle$$

and $$\langle I(m)\rangle = \langle V_m(t)V_m^*(t)\rangle \quad .$$

For a plane wave reference beam, $\langle I(R)\rangle = \langle I_R(P)\rangle$, the irradiance at P due to the reference beam.

The complex degree of coherence can now be written as

$$\gamma_{Rm}(\tau_{mRP}) = \frac{\langle V_R(t)V_m^*(t-\tau_{mRP})\rangle}{\left[\langle I(R)\rangle\langle I(m)\rangle\right]^{\frac{1}{2}}} \quad . \qquad (3-5)$$

Substituting Eqn. 3-5 into Eqn. 3-3 yields

$$\mathrm{Re}\langle V_{RP}(t)V_{mP}^*(t)\rangle = \frac{1}{g(s_{mP})}\left[\langle I(R)\rangle\langle I(m)\rangle\right]^{\frac{1}{2}}\mathrm{Re}\,\gamma_{Rm}(\tau_{mRP}) \quad . \qquad (3-6)$$

This can be expressed in a more meaningful form by the substitutions below.

Let us assume that the magnitude of the radiation leaving the reference beam source and the object are both constant in time. Then we can write

$$V_R(t) = A_R e^{j\omega t}$$

and $$V_m(t) = A_m e^{j(\omega t+\theta_m)}$$

where θ_m accounts for the fact that radiation from different parts of the object can have different phases. For example, for a reflecting object, θ_m would depend on the distance from the illuminating source to m. From

these expressions we find

$$\langle V_R(t) V_m^*(t-\tau_{mRP}) \rangle = \langle A_R A_m e^{j(\omega\tau_{mRP} - \theta_m)} \rangle$$

$$= A_R A_m e^{j(\omega\tau_{mRP} - \theta_m)} . \qquad (3-7)$$

Strictly, ω is a function of time since we are considering radiation that is varying randomly within a frequency range limited to $\omega \pm \frac{1}{2}\Delta\omega$. In general then, $e^{j\omega\tau_{mRP}}$ may not be constant. However, we are restricting this discussion to q-m light, for which

$$\tau_{mRP} \ll 1/\Delta\omega,$$

so that even at the moment of maximum variation from the center frequency ω,

$$e^{j(\omega \pm \frac{1}{2}\Delta\omega)\tau_{mRP}} = e^{j\omega\tau_{mRP}} e^{\pm j\frac{1}{2}\Delta\omega\tau_{mRP}}$$

$$\cong e^{j\omega\tau_{mRP}}$$

since $\frac{1}{2}\Delta\omega\tau_{mRP} \ll 1$. Therefore,

$$\langle e^{j\omega\tau_{mRP}} \rangle \cong e^{j\omega\tau_{mRP}} .$$

For similar reasons, although θ_m may also be a function of time, in the following we will also assume that

$$\langle e^{j\theta_m} \rangle \cong e^{j\theta_m} .$$

Substituting Eqn. 3-7 into Eqn. 3-5, we obtain,

$$\mathrm{Re}\gamma_{Rm}(\tau_{mRP}) = \left|\gamma_{Rm}(\tau_{mRP})\right| \cos(\omega\tau_{mRP}-\theta_m) \quad . \qquad (3\text{-}8)$$

Using Eqns. 3-8 and 3-6 in 3-2, we have finally

$$\langle I(P)\rangle = \langle I_o(P)\rangle + \langle I_R(P)\rangle + 2\left[\langle I(R)\rangle\right]^{\frac{1}{2}} \times \sum_m A_m \frac{1}{g(s_{mP})} \left|\gamma_{Rm}(\tau_{mRP})\right| \cos(\omega\tau_{mRP}-\theta_m). \qquad (3\text{-}9)$$

where we have used the fact that

$$\langle I(m)\rangle = \langle V_m(t)V_m^*(t)\rangle = A_m^2 \quad .$$

$\langle I(P)\rangle$ in Eqn. 3-9 is the time average irradiance at the point P on the plane H. A photographic plate exposed to $\langle I(P)\rangle$ becomes a hologram. Assume for simplicity that the plate is processed to produce a positive transparency with amplitude transmittance proportional to $\langle I(P)\rangle$.* If the processed plate is illuminated with a source identical

---

*Strictly speaking, this requires a positive plate with overall gamma (not to be confused with coherence) of -2 since, for such a plate exposed to an average irradiance $\langle I(P)\rangle$ for a time T

$$\gamma \log\left[\langle I(P)\rangle T\right] = \log \frac{\text{incident flux}}{\text{transmitted flux}}$$

$$\log\left[\langle I(P)\rangle T\right] = -\tfrac{1}{2}\log \frac{\text{incident flux}}{\text{transmitted flux}}$$

$$= \log \frac{\text{transmitted amplitude}}{\text{incident amplitude}} \quad .$$

However, holograms can be made with other values of gamma and are, in fact, usually made with negative plates developed to gamma's of 6 or more.

to the reference source (but with amplitude V_i) positioned as it was in Fig. 3-1, then at the hologram plane, the analytic signal of the incident radiation is

$$V_i \cos\omega(t - s_{RP}/c)$$

and the analytic signal of the transmitted radiation is

$$V_i \langle I(P)\rangle \cos\,\omega(t - s_{RP}/c) \quad . \qquad (3\text{-}10)$$

Substituting $\langle I(P)\rangle$ from Eqn. 3-9 into Eqn. 3-10 shows that the resulting expression contains three terms. Each of these represents an analytic signal which will result in a wave emerging from the plate. The waves produced by the first two terms are approximately plane waves of no apparent interest. However, the third term is

$$2V_i\left[\langle I(R)\rangle\right]^{\frac{1}{2}} \sum_m \frac{1}{q(s_{mP})} A_m \left|\gamma_{Rm}(\tau_{mRP})\right| \cos(\omega\tau_{mRP} - \theta_m)\cos\,\omega(t - \tfrac{s_{RP}}{c})$$

$$= V_i\left[\langle I(R)\rangle\right]^{\frac{1}{2}} \sum_m \frac{1}{q(s_{mP})} A_m \left|\gamma_{Rm}(\tau_{mRP})\right| \left\{\cos\left[\omega(t - \tfrac{s_{RP}}{c} + \tau_{mRP}) - \theta_m\right] + \cos\left[\omega(t - \tfrac{s_{RP}}{c} - \tau_{mRP}) + \theta_m\right]\right\}$$

$$= U(P,t)_+ + U(P,t)_-$$

or,

$$U(P,t)_\pm = V_i\left[\langle I(R)\rangle\right]^{\frac{1}{2}} \sum_m \frac{1}{q(s_{mP})} A_m \left|\gamma_{Rm}(\tau_{mRP})\right| \cos\left[\omega(t - \tfrac{s_{RP}}{c} \pm \tau_{mRP}) \mp \theta_m\right] \qquad (3\text{-}11)$$

$$\tau_{mRP} = \frac{s_{mP} - s_{RP}}{c} \quad .$$

The significance of $U(P,t)_{\pm}$ is most easily seen by comparing it with $W(P,t)$, the analytic signal that would be produced at the plane H by the object alone, illuminated exactly as it was when the hologram was made. From Fig. 3-2 this is clearly

$$W(P,t) = \sum_m \frac{1}{g(s_{mP})} A_m \cos\left[\omega\left(t - \frac{s_{mP}}{c}\right) + \theta_m\right] . \quad (3\text{-}12)$$

Notice that $U(P,t)_-$ differs from $W(P,t)$ only by the amplitude multipliers $V_i \left[\langle I(R)\rangle\right]^{\frac{1}{2}} \left|\gamma_{Rm}(\tau_{mRP})\right|$.

$W(P,t)$ is the analytic signal that can produce an image of the object. It is generated by the superposition of spherical waves of appropriate amplitudes from each infinitesimal element of the object. Therefore, $U(P,t)_-$ is also a summation of spherical waves from each element of the object (or, more precisely, appearing to be from each element of the object) and can produce a clear, undistorted image of the object. However, the amplitude of the signal from each element m is altered by the amplitude multiplier. The portion $V_i\left[\langle I(R)\rangle\right]^{\frac{1}{2}}$ is constant and shows only that the overall amplitude of the reconstructed signal depends on the amplitudes of the reconstructing and reference beams. But $\left|\gamma_{Rm}(\tau_{mRP})\right|$ is not constant, and may affect the relative amplitudes of different

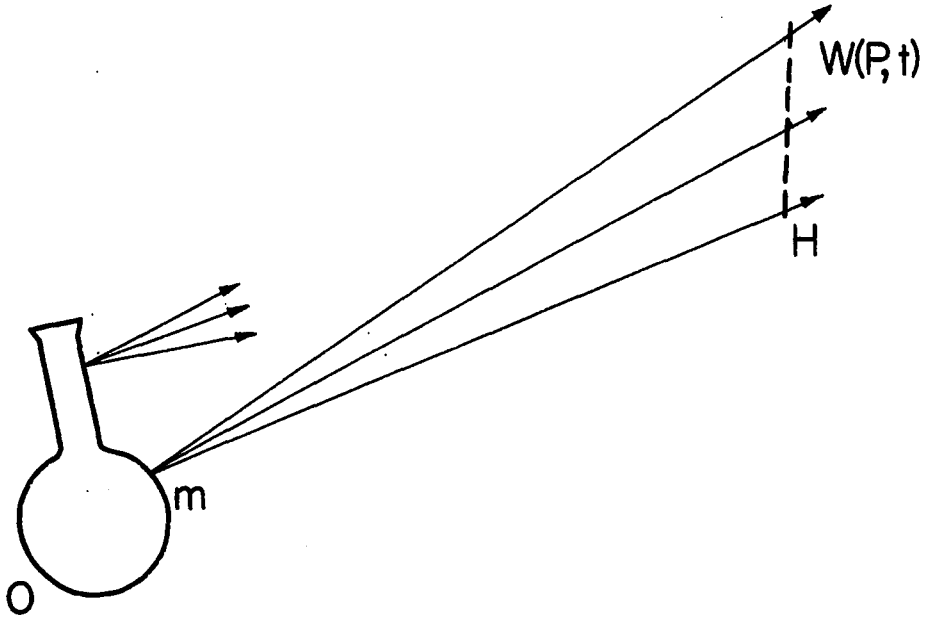

Figure 3-2. W(P,t) is the analytic signal at the plane H, due to the illuminated object alone.

portions of the signal, thereby changing any image reconstructed from $U(P,t)_-$. Inspection of our definition in Eqn. 3-4 shows that $\gamma_{Rm}(\tau_{mRP})$ depends on m and on s_{mP} because of the definition of τ_{mRP}. However, by the definition of q-m radiation, the magnitude of the coherence does not vary appreciably over distances of the order of the variations in s_{mP} in our system. Therefore, the magnitude of the coherence in this case is independent of τ_{mRP} and is a function only of m. In fact we may write

$$\left|\gamma_{Rm}(\tau_{mRP})\right| = \left|\gamma_{Rm}(0)\right|$$

for q-m radiation.

We conclude that $U(P,t)_-$ is an analytic signal that represents a wave that seems to be coming from an object O, except that the amplitude of the radiation from each element m of the object appears to be multiplied by $\left|\gamma_{Rm}(0)\right|$. An observer or optical instrument viewing the wave $U(P,t)_-$ will see a clear reconstruction of O having an intensity shaded in proportion to $\left|\gamma_{Rm}(0)\right|^2$.*

---

*It can also be shown by a similar discussion that $U(P,t)_+$ reconstructs a real image of O having the same dependence on $\left|\gamma_{Rm}(0)\right|$ as the virtual image reconstructed by $U(P,t)_-$.

In Chapter 4 a method for measuring coherence is developed, based on this result.

3.2. Fourier Transform Holograms with Partially Coherent Light, a Special Case[2]

3.2.1. The virtual images reconstructed by a Fourier transform hologram. In the preceding section, we assumed that the reference and reconstructing beams were plane waves. We will now show that similar results are obtained with another particularly important geometry, namely an arrangement in which the reference beam comes from a point (or very small) source located at approximately the same distance from the hologram plane as the object, as indicated in Fig. 3-3. Stroke et.al.[3] and Winthrop and Worthington[4] have shown that for this situation the irradiance on the hologram plane is the spatial Fourier transform of the light distribution at the object. Such a hologram is called a Fourier transform hologram. In Appendix I we show that this same type of hologram will be produced by a plane wave reference beam and an object at infinity. Fourier transform holograms generally involve lower spatial frequencies than Fresnel holograms because the angles between the interfering beams

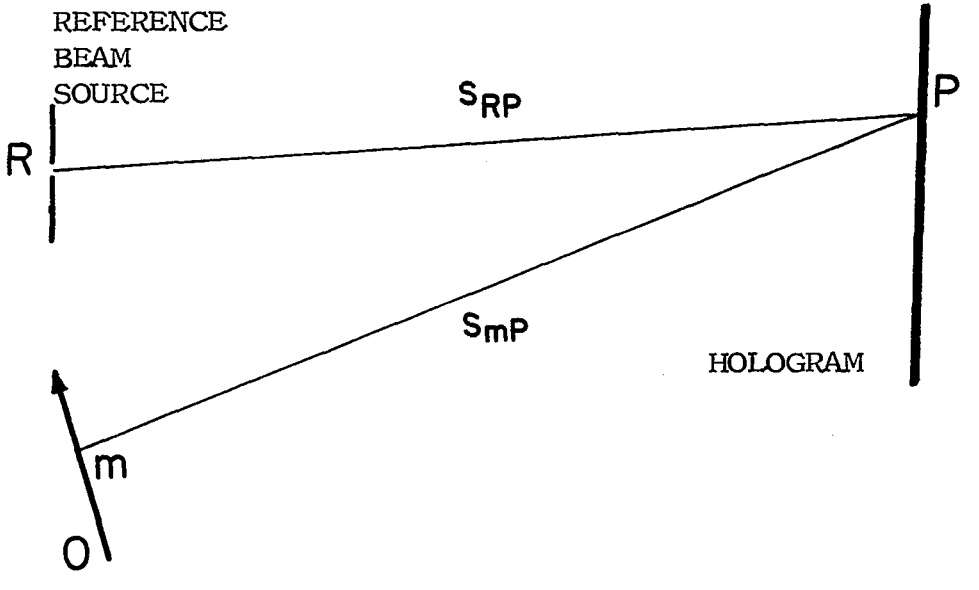

Figure 3-3. An arrangement for producing a Fourier transform hologram of an object O. The illumination of the object can have any degree of spatial coherence, but the reference beam, coming from the very small, quasi-monochromatic source R, must be highly coherent. The distance from any point m on the object to any point P on the hologram is s_{mP}; the distance from the reference source R to P is s_{RP}.

are smaller. This permits the use of film with lower spatial frequency response (lower resolution) and, consequently, greater speed. This is especially important in experiments involving low light intensities, notably the coherence measurements described in Chapter 4. Secondly, the arrangement shown in Fig. 3-3, which yields this type of hologram, is often easier to construct than the system required for Fresnel holograms, such as the system shown in Fig. 1-2. To produce a Fourier transform hologram, one needs only the appropriately illuminated object and a point reference source near the object. The more closely one meets the condition that the points on the object are at the same distance from the hologram as the reference source, the better the approximation to a perfect Fourier transform hologram. There is always some approximation involved since, except for a point object and a point hologram, the distances from the hologram to the object and to the reference beam will vary over the object and over the hologram.

Let $V_R(t)$ and $V_m(t)$ be the analytic signals at the reference source R and at the element m of the object, respectively. Let $V_{RP}(t)$ and $V_{mP}(t)$ be the analytic

signals at P due to $V_R(t)$ and $V_m(t)$, respectively. Then, following the reasoning in Section 3.1, if I(P) is the irradiance at P,

$$\langle I(P)\rangle = \tag{3-13}$$

$$\langle I_o(P)\rangle + \langle I_R(P)\rangle + 2\sum_m \mathrm{Re}\langle V_{RP}(t)\, V_{mP}^*(t)\rangle$$

where $I_o(P)$ is the irradiance that would be produced at P by all the radiation from the object O without the reference beam, and $I_R(P)$ is the irradiance that would be produced at P by the reference beam without the object. Referring to Fig. 3-3,

$$V_{mP}(t) = \frac{1}{g(s_{mP})}\, V_m\left(t - \frac{s_{mP}}{c}\right)$$

and

$$V_{RP}(t) = \frac{1}{g'(s_{RP})}\, V_R\left(t - \frac{s_{RP}}{c}\right)$$

where the functions g and g' are defined as in Chapter 2. Then

$$\langle V_{RP}(t)\, V_{mP}^*(t)\rangle =$$

$$\frac{1}{g(s_{mP})\, g'(s_{RP})}\left\langle V_R\left(t - \frac{s_{RP}}{c}\right) V_m^*\left(t - \frac{s_{mP}}{c}\right)\right\rangle =$$

$$\frac{1}{g(s_{mP})\, g'(s_{RP})}\left\langle V_R(t)\, V_m^*(t - \tau_{mRP})\right\rangle \tag{3-14}$$

where $\tau_{mRP} = \dfrac{s_{mP} - s_{RP}}{c}$.

By the definitions in Eqns. 2-1 and 2-3

$$\gamma_{Rm}(\tau_{mRP}) = \frac{\langle V_R(t+\tau_{mRP})V_m^*(t)\rangle}{[\langle V_R(t)V_R^*(t)\rangle \langle V_m(t)V_m^*(t)\rangle]^{\frac{1}{2}}}$$

is the coherence of the radiation at m measured with respect to the radiation at the source R of the reference beam. Letting

$$\langle I(R)\rangle = \langle V_R(t)V_R^*(t)\rangle$$

and

$$\langle I(m)\rangle = \langle V_m(t)V_m^*(t)\rangle$$

and shifting the time origin,

$$\gamma_{Rm}(\tau_{mRP}) = \frac{\langle V_R(t)V_m^*(t-\tau_{mRP})\rangle}{[\langle I(R)\rangle \langle I(m)\rangle]^{\frac{1}{2}}} . \qquad (3\text{-}15)$$

Introducing Eqns. 3-15 and 3-14 into 3-13, we obtain

$$\langle I(P)\rangle = \langle I_o(P)\rangle + \langle I_R(P)\rangle + \qquad (3\text{-}16)$$

$$\frac{2}{q'(S_{RP})}[\langle I(R)\rangle]^{\frac{1}{2}} \sum_m \frac{1}{q(S_{mP})}[\langle I(m)\rangle]^{\frac{1}{2}} Re\,\gamma_{Rm}(\tau_{mRP}).$$

As in the previous section, we can write

$$Re\gamma_{Rm}(\tau_{mRP}) = |\gamma_{Rm}(\tau_{mRP})| \cos(\omega\tau_{mRP} - \theta_m)$$

where θ_m is a constant independent of P for any given m. Substituting this into Eqn. 3-16 gives for the time average irradiance at P on the hologram plane H

$$\langle I(P)\rangle = \langle I_o(P)\rangle + \langle I_R(P)\rangle + \qquad (3\text{-}17)$$

$$\frac{2}{g'(s_{RP})}\left[\langle I(R)\rangle\right]^{\frac{1}{2}} \sum_m \frac{1}{g(s_{mP})}\left[\langle I(m)\rangle\right]^{\frac{1}{2}} \left|\gamma_{Rm}(\tau_{mRP})\right| \cos(\omega\tau_{mRP} - \theta_m).$$

If a photographic plate is exposed to this irradiance, then processed so that its amplitude transmittance is proportional to $\langle I(P)\rangle$, and finally illuminated with a reconstructing beam that is of the same form as the reference beam, namely

$$\frac{1}{g'(s_{RP})} V_i \cos \omega\left(t - \frac{s_{RP}}{c}\right),$$

then the transmitted wave will be proportional to

$$\frac{1}{g'(s_{RP})} V_i \langle I(P)\rangle \cos \omega\left(t - \frac{s_{RP}}{c}\right). \qquad (3\text{-}18)$$

Again we are interested in the term in the expansion of Eqn. 3-18 that reconstructs images of O, namely

$$\frac{2}{g'(s_{RP})} V_i \left[\langle I(R)\rangle\right]^{\frac{1}{2}}$$

$$\times \sum_m \frac{1}{g(s_{mP})}\left[\langle I(m)\rangle\right]^{\frac{1}{2}} \left|\gamma_{Rm}(\tau_{mRP})\right| \cos(\omega\tau_{mRP} - \theta_m) \cos\left[\omega\left(t - \frac{s_{RP}}{c}\right)\right].$$

Since $\tau_{mRP} = (s_{mP} - s_{RP})/c$, this can be written as

$$\frac{1}{g'(s_{RP})} V_i \left[\langle I(R)\rangle\right]^{\frac{1}{2}}$$

$$\times \sum_m \frac{1}{g(s_{mP})} \left[\langle I(m)\rangle\right]^{\frac{1}{2}} \left|\gamma_{Rm}(\tau_{mRP})\right| \left\{\cos\left[\omega\left(t + \frac{s_{mP}}{c} - \frac{2s_{RP}}{c}\right) - \theta_m\right]\right.$$

$$\left. + \cos\left[\omega\left(t - \frac{s_{mP}}{c}\right) + \theta_m\right]\right\}$$

$$= U(P,t)_+ + U(P,t)_- \quad .$$

More compactly,

$$U(P,t)_\pm = \frac{1}{g'(s_{RP})} V_i \left[\langle I(R)\rangle\right]^{\frac{1}{2}}$$

$$\times \sum_m \frac{1}{g(s_{mP})} A_m \left|\gamma_{Rm}(\tau_{mRP})\right| \cos\left[\omega\left(t \pm \frac{s_{mP}}{c} - \frac{s_{RP}}{c} \mp \frac{s_{RP}}{c}\right) \mp \theta_m\right] \qquad (3\text{-}19)$$

where we have used

$$\langle I(m)\rangle = \langle V_m(t) V_m^*(t)\rangle = A_m^2$$

for $V_m(t)$ having a constant amplitude A_m.

$U(P,t)_-$ is again similar to $W(P,t)$ in Eqn. 3-12 which we rewrite here:

$$W(P,t) = \sum_m \frac{1}{g(s_{mP})} A_m \cos\left[\omega\left(t - \frac{s_{mP}}{c}\right) + \theta_m\right]. \qquad (3\text{-}20)$$

The amplitude of $U(P,t)_-$ depends not only on the constant multiplier $\frac{1}{g'(sRP)} V_i \left[\langle I(R)\rangle\right]^{\frac{1}{2}}$, but also on the variable

term $\left|\gamma_{Rm}(\tau_{mRP})\right|$.

Assume for the moment that $\left|\gamma_{Rm}(\tau_{mRP})\right| = 1$ so we can discuss the effect of $1/g'(s_{RP})$ alone. Figure 3-2 illustrated the formation of W(P,t) by the object. In that figure, imagine a gray filter (attenuator) placed in the plane H and having an amplitude transmittance that varied with P as $1/g'(s_{RP})$. The wave at the right of the plane H would then be

$$W'(P,t) = \frac{1}{g'(s_{RP})} \sum_m \frac{1}{g(s_{mP})} A_m \cos\left[\omega\left(t - \frac{s_{mP}}{c}\right) + \theta_m\right].$$

This shows that U(P,t)_ will reconstruct an image of the object as if it were being viewed through a shaded filter placed at the hologram plane as above. Because $g'(s_{RP})$ varies very little over the surface of the hologram, as discussed in Chapter 2, this effect can be ignored in practice. If necessary, it could be completely eliminated by simply placing a suitable compensating filter behind the hologram during the reconstruction process as is common practice in rear screen projection equipment.

Let us return now to the more important term $\left|\gamma_{Rm}(\tau_{mRP})\right|$. Using the q-m approximation (i.e. for sufficiently small τ_{mRP}) we find that

$$\left|\gamma_{Rm}(\tau_{mRP})\right| = \left|\gamma_{Rm}(0)\right|$$

which is constant for each m and so affects the amplitude, but not the sphericity of the wave from each element m.

We have shown, therefore, that the wave represented by $U(P,t)_-$ reconstructed by a Fourier transform hologram produces a virtual image of an object in which the amplitude of the wave at each element m of the object is multiplied by $\left|\gamma_{Rm}(0)\right|$. Thus the Fourier transform hologram made with a spherical reference beam produces the same virtual image as the hologram made with a plane wave reference beam.

The phase of $U(P,t)_+$ is $\frac{\omega}{c}(s_{mP}-2s_{RP})-\theta_m$. We will now show that this is the phase distribution that is produced by an inverted mirror image of the object, provided the dimensions of the hologram and of the area occupied by the object and the reference source R are all small compared to $\bar{R}$, the distance from R to the center of the hologram.

Let the reference source R, a point m on the object, and the hologram H be arranged as in Fig. 3-4. The phase of the light reaching P from m is $-\frac{\omega}{c}s_{mP}$, relative to the

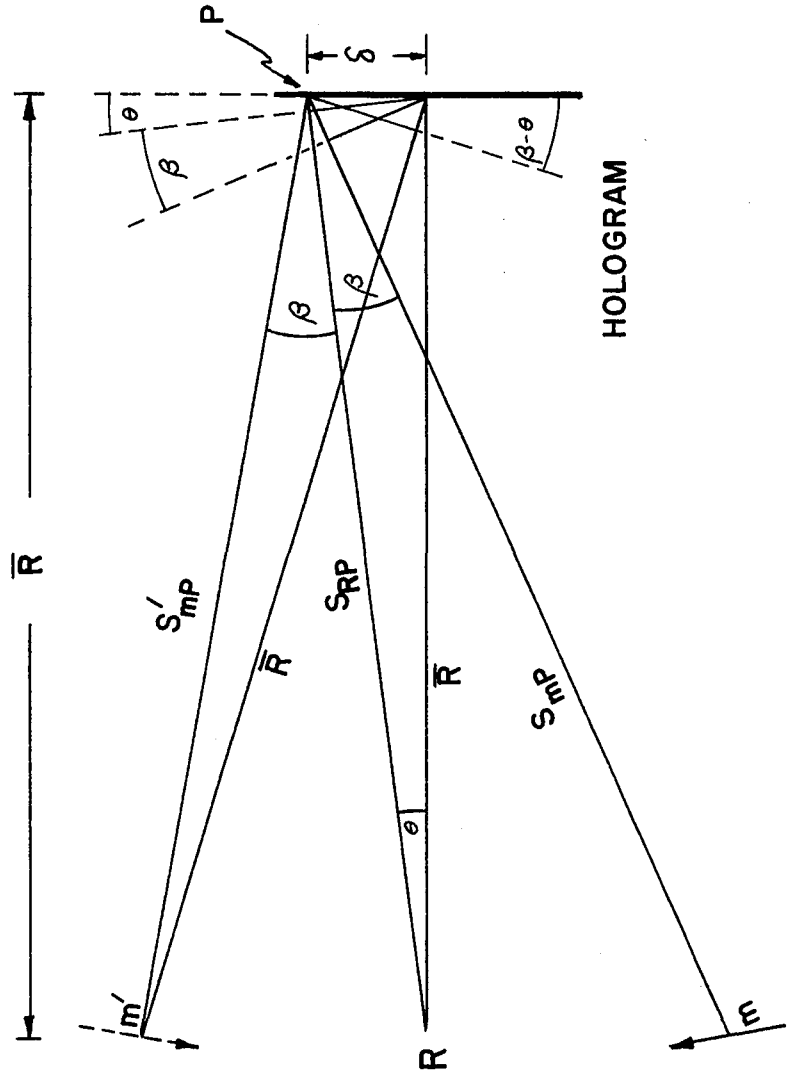

Figure 3-4. The geometry used to demonstrate that U(P,t)_ reconstructs an inverted mirror image of the object.

phase at m. Let m' be a source radiating synchronously with m and located symmetrically to m with respect to R as in the figure. Then $-\frac{\omega}{c}s_{mP}$ is the phase of the light reaching P from m'. Since β is a small angle and δ is a small displacement because of the restrictions on the dimensions in the figure, we can approximate

$$s_{RP} \cong \bar{R} + \delta\sin\theta$$

$$s_{mP} \cong \bar{R} + \delta\sin(\beta+\theta)$$

and $$s'_{mP} \cong \bar{R} - \delta\sin(\beta-\theta) \quad .$$

Since the hologram is generally smaller than the object, we can assume that θ is restricted to even smaller values than β. Then

$$\sin(\beta+\theta) \cong \theta + \sin\beta$$

and $$\sin(\beta-\theta) \cong -\theta + \sin\beta \ .$$

Therefore,

$$\begin{aligned} s'_{mP} &= \bar{R} - \delta\sin\beta + \delta\theta \\ &= 2\bar{R} + 2\delta\theta - (\bar{R} + \delta\theta + \delta\sin\beta) \\ &= 2s_{RP} - s_{mP} \ . \end{aligned}$$

The phase of $U(P,t)_+$ can now be written in terms of s'_{mP} as

$$\frac{\omega}{c}(s_{mP}-2s_{RP}) - \theta_m = -s'_{mP}\frac{\omega}{c} - \theta_m$$

so that

$$U(P,t)_{+} = \frac{1}{g'(s_{RP})} V_i \left[\langle I(R)\rangle\right]^{\frac{1}{2}}$$

$$\times \sum_{m} \frac{1}{g(s_{mP})} A_m \left|\gamma_{Rm}(0)\right| \cos\left[\omega\left(t - \frac{s'_{mP}}{c}\right) - \theta_m\right] \quad (3\text{-}21)$$

when the approximations above are valid. In that case, $U(P,t)_{+}$ reconstructs an image made up of the points such as m' in Fig. 3-4. From the symmetry of that figure it is clear that the resulting image is inverted and reversed left-to-right (mirror) with respect to the object O. The amplitude of the radiation from each point m' is multiplied by the same factor as for the corresponding point in $U(P,t)_{-}$ so the image formed by $U(P,t)_{+}$ shows the same intensity variations as the image formed by $U(P,t)_{-}$.

Of course, the preceding analysis requires each m to be at the distance $\overline{R}$ from the center of the hologram, a condition which generally cannot be met. As a result of this, the conjugate image reconstructed by the Fourier transform hologram is described only approximately by this analysis. Notice, however, that the image produced by $U(P,t)_{-}$ is always an accurate reproduction of the object.

3.2.2. Reconstruction of a real image from a Fourier transform hologram. To produce a real image of an object O from a Fourier transform hologram, we must reconstruct waves that converge to points distributed in space in the same way as the points m that make up the actual object O. That is, whereas the radiation from the object consists of a summation of spherical waves coming from the points m of the object, the real image consists of waves converging to points having a distribution in space that is the same as (or closely related to) the distribution of the points m. If a screen is positioned so that the image points lie on the screen, the converging rays will produce a projected (real) image on it. If the screen is replaced by a photographic emulsion, a recording of the image can be made: lensless photography. Of course, if the object was three-dimensional, the image points would be distributed over three dimensions so that they could not be positioned on the screen simultaneously. Therefore, parts of the image on the screen would be out of focus. This is very similar to the problem of depth of focus with conventional imaging methods (e. g. lenses).

Consider the hologram H, with amplitude transmittance

$\langle I(P)\rangle$ given by Eqn. 3-17, and illuminated by coherent light focussed on the point F as in Fig. 3-5. Since this light is propagating to the right as spherical waves converging towards F, the wave reaching any point P on the hologram is represented by

$$A(P)\cos\ \omega(t + s_{PF}/c) \qquad (3\text{-}22)$$

where the amplitude is some function of P depending on the optical system used to produce the reconstructing beam and where, to make the convergence of the beam to F most explicit, the phase is measured with respect to the phase that the radiation will have at F. s_{PF} is the distance between any point P on the hologram and the point F. The wave transmitted by the hologram in this case is

$$A(P)\langle I(P)\rangle \cos\ \omega(t + s_{PF}/c)\ . \qquad (3\text{-}23)$$

Notice that the only differences between Eqns. 3-23 and 3-18 which produced the virtual images are that $[1/g'(s_{RP})]V_i$ is replaced by A(P) and $\omega(t - s_{RP}/c)$ is replaced by $\omega(t + s_{PF}/c)$. Therefore, we can apply the results of the previous discussion, namely Eqn. 3-19, to the present problem. The system in Fig. 3-5 accordingly produces two waves

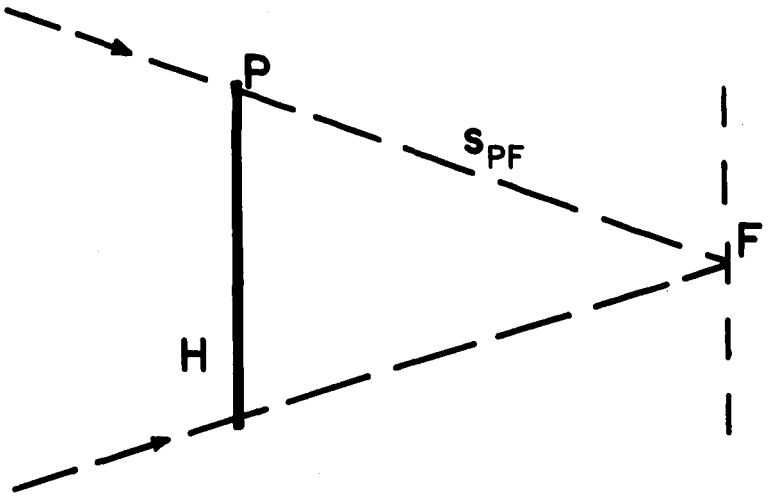

Figure 3-5. Reconstruction of a real image from a Fourier transform hologram H using a reconstructing beam that converges to the point F and is the conjugate of the reference beam, i.e. has phase with opposite sign. A planar object will produce a pair of real images in a plane containing the point F.

$$V(P,t)_{\pm} = \frac{1}{q'(s_{RP})} A(P)\left[\langle I(R)\rangle\right]^{\frac{1}{2}} \qquad (3\text{-}24)$$

$$\times \sum_{m} \left\{ \frac{1}{q(s_{mP})} A_m \left| \gamma_{Rm}(o) \right| \right.$$

$$\left. \times \cos\left[\omega\left(t \pm \frac{s_{mP}}{c} + \frac{s_{PF}}{c} \mp \frac{s_{RP}}{c}\right) \mp \theta_m\right] \right\} .$$

If s_{PF} in the arrangement illustrated in Fig. 3-5, is made equal to s_{RP}, the argument of each term in $V(P,t)_+$ is $\omega(t + s_{mP/c}) - \theta_m$. By comparison with Eqn. 3-22, each of these terms represents a spherical wave propagating to the right from the plane H and converging to a point at a distance s_{mP} to the right of each point P of the hologram. From this it is evident that for each point m on the object, which was to the left of the hologram when it was exposed, there will be a corresponding real image point located symmetrically to the right of the hologram. Call each of these image points m''. The m'' determined in this manner combine to form the real image of O. The waves arriving at the points m'' have relative phases given by θ_m which are the same as the relative phases of the waves that originated at the corresponding points of the object.

From Eqn. 3-24 we see that the amplitude at each point m'' of the image is equal to the amplitude of the corresponding point m of the object multiplied by

$$\frac{1}{g'(s_{RP})} A(P)\left[\langle I(R)\rangle\right]^{\frac{1}{2}} \left| \gamma_{Rm}(o) \right| \quad .$$

The factor $\frac{1}{g'(s_{RP})} A(P) \left[\langle I(R)\rangle\right]^{\frac{1}{2}}$ is independent of m, and as shown previously, does not appreciably affect the amplitude of the light forming the image of m in the reconstruction. Therefore, this real image, produced by a Fourier transform hologram using the arrangement shown in Fig. 3-5, shows the same dependence on coherence as the virtual image. That is, the amplitude at the point m'' of the image, corresponding to the point m of the object, is proportional to $\left| \gamma_{Rm}(0) \right|$.

If $V(P,t)_-$ is analyzed, it is found to produce a real image that is inverted and reversed left to right with respect to that produced by $V(P,t)_+$, as we might expect from the previous results.

REFERENCES

1. Portions of the work in this section have been published by this author. See
M. Lurie, J.Opt.Soc.Am. 56, 1369 (1966).
2. Portions of the work in this section have been submitted for publication in the J.Opt.Soc.Am..
3. G. W. Stroke, D. Brumm and A. Funkhouser, J.Opt.Soc.Am. 55, 1327 (1965).
4. J. T. Winthrop and C. R. Worthington, Phys. Letters 15, 124 (1965).

CHAPTER IV

HOLOGRAPHIC MEASUREMENT OF SPATIAL COHERENCE

The theoretical results of Chapter 3 suggest that a hologram could be used to measure spatial coherence by simply measuring the irradiance of an appropriate reconstructed image. The use of this method is described below and the results of a measurement of coherence are compared with theoretical values.

In order to check the measured values of coherence, it was necessary to construct a system which illuminated an object with partially coherent light whose degree of coherence could be calculated. Section 4.1 treats the problem of producing this illumination and calculating its coherence. The following sections describe the apparatus used to produce the hologram and discuss the results of a measurement of spatial coherence.

4.1. Production of Quasi-monochromatic Light with Known Spatial Coherence

The results of Chapter 3, in particular Eqn. 3-24, are valid only for q-m light. Light of a suitably narrow bandwidth is most easily produced with a laser. However,

we require q-m light of varying spatial coherence whereas laser light has almost complete spatial coherence, i.e. $|\gamma(0)| = 1$. The required light can be produced by completely destroying the spatial coherence of a laser beam and then restoring it to the desired degree.

As illustrated schematically in Fig. 4-1, a He-Ne laser beam of just under 1 mW is concentrated - but not brought to a sharp focus - on a piece of rotating ground glass G. This randomizes the phase, destroying the spatial coherence and illuminating the condensing lenses C with incoherent q-m light, provided the concentrated spot on the ground glass is large enough to assure that the area of coherence of the light from that spot is much smaller than the condenser aperture (see Section 2.3). This would seem to be an important consideration when using this common technique for destroying coherence, since there is a temptation to focus the laser beam sharply on the ground glass to produce the most intense spot. Using a very small spot defeats the purpose, however, since the transmitted light appears highly coherent at even small distances from the ground glass because the focussed spot forms such a small source. Furthermore,

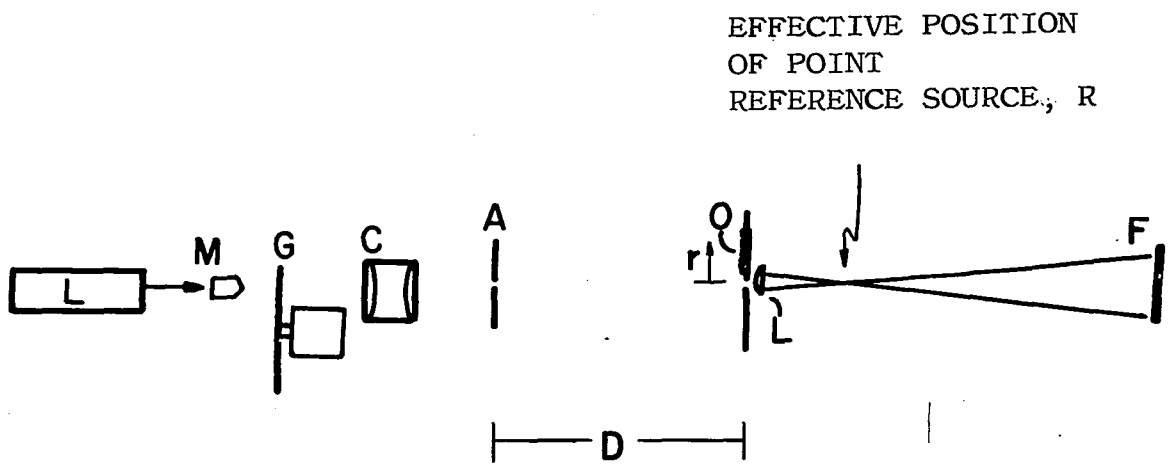

Figure 4-1. Equipment for illuminating an object with partially coherent, quasi-monochromatic light and taking a hologram of the object. The rotating ground glass G destroys the spatial coherence of the output of the laser L. Therefore, the coherence of the light reaching the object O from the small circular aperture A is easily calculated and has the form of the familiar Airy pattern. A portion of the light near the optical axis passes through another aperture near the object and then through a 3 mm focal length lens L and is used for the reference beam. M is a microscope objective, C is a condensing lens and F is the film to record the hologram.

consideration must be given to the grain size of the ground glass. Only if the focussed spot covers many grains is it reasonable to state that the motion of the ground glass randomizes the phase of the transmitted radiation. If the spot is smaller than the size of a grain, then the effect of moving the ground glass will be a pulsation of the phase with relatively long periods of almost constant phase during the time that one grain moves in front of the focussed spot. Clearly, this will not result in zero spatial coherence.

With the above precaution, however, the condensing lenses illuminate the circular aperture A with incoherent, q-m light. Aperture A can then be considered as a circular, incoherent, q-m source. It illuminates the plane containing the object O with partially coherent light. The degree of coherence of this light varies in accordance with the van Cittert-Zernike theorem given in Eqn. 2-11 and repeated here:

$$|\gamma_{12}(\tau)| = \left|\frac{2J_1(v)}{v}\right| \qquad (4\text{-}1)$$

$$= |\gamma_{12}(0)| = |\gamma_r(0)| \qquad (4\text{-}2)$$

where $v = \frac{\omega}{c}(\frac{\rho}{D})r$,

ρ = radius of the circular aperture A,

D = distance from the aperture A to the plane of the object O, and

r = distance between the points 1 and 2 for which the coherence is being determined. This was $\overline{P_1P_2}$ in the notation of Chapter 2.

In the apparatus illustrated in Fig. 4-1,

$$\rho = 0.0077 \text{ mm}$$

$$D = 30 \text{ cm}$$

$$\frac{\omega}{c} = \frac{2\pi}{\lambda} = \frac{2\pi}{633 \text{ nm}}$$

which gives $v = 0.257r$ for r in mm.

We can calculate the coherence of the light from A reaching any point in the plane of the object with respect to the light at the point Q at the center of the object, i.e at the intersection of the plane of the object with r = 0 at Q, as indicated in Fig. 4-2 and also in Fig. 4-1. More details are discussed in Section 4.2. The magnitude of the coherence as a function of r, calculated according to

$$|\gamma_r(0)| = \left|\frac{2J_1(v)}{v}\right| \qquad (4\text{-}3)$$

is shown in Fig. 4-3. All possible values of coherence, from 0 to 1, are provided by this procedure.

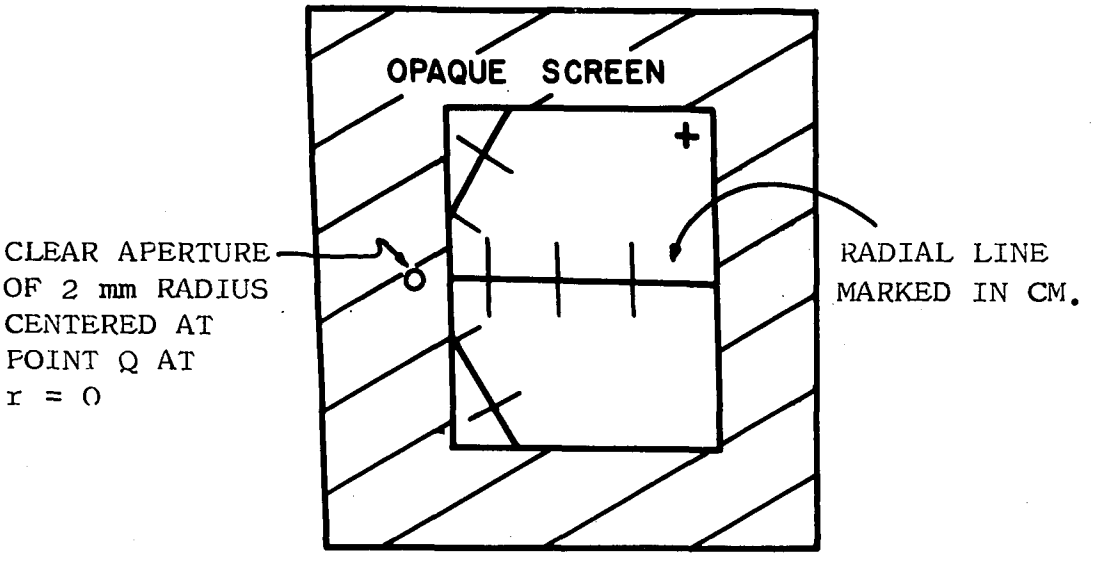

Figure 4-2. A drawing of the object O which is a 1.4 X 1.8 inch piece of ground glass with radial lines originating on the optical axis and marked in cm. A small aperture Q, centered on the axis near the edge of the object, allows a highly coherent wave to pass undiffused. This is spread by means of a 3 cm focal length lens and forms the reference beam.

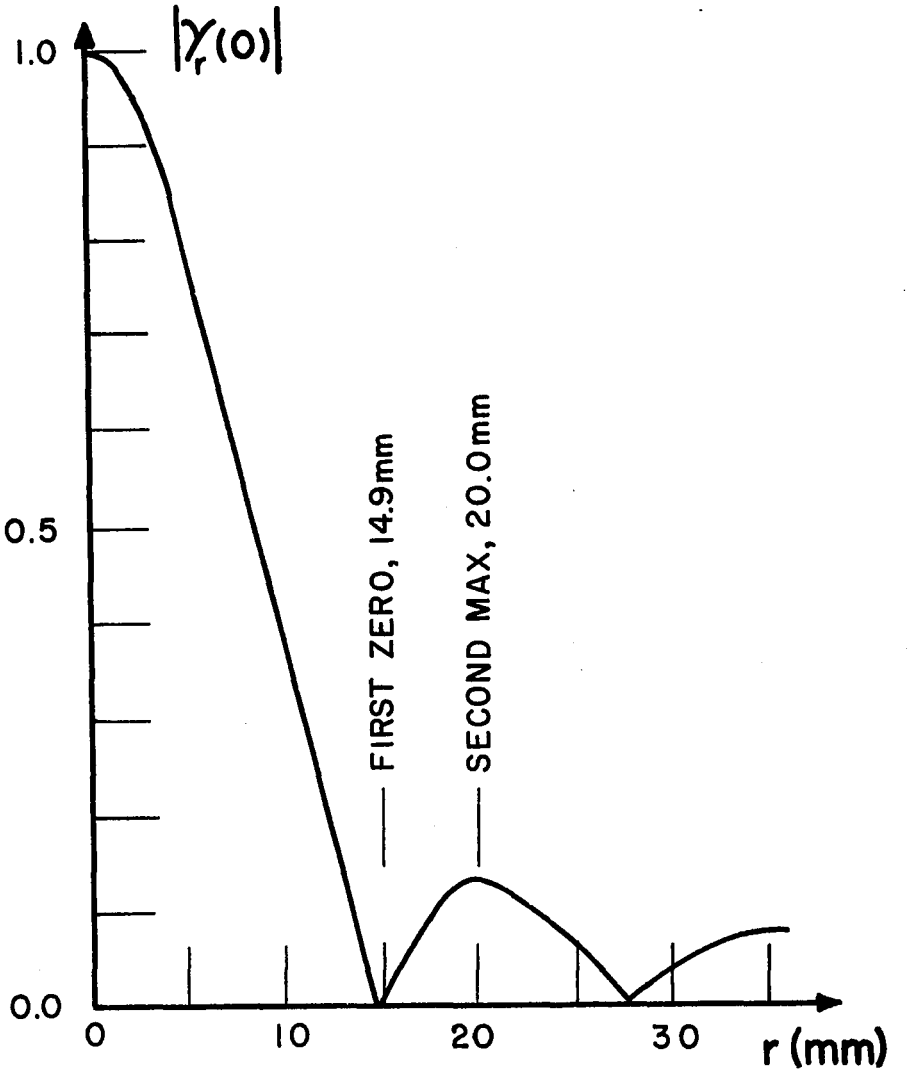

Figure 4-3. The magnitude of the degree of coherence of the light reaching the object in the apparatus shown in Fig. 4-1, as a function of r, the distance from the optical axis, calculated according to the van Cittert-Zernike theorem.

4.2. Description of Apparatus for Producing a Hologram of an Object Illuminated with Partially Coherent Light

We saw in the previous section that the plane of the object O in Fig. 4-1 is illuminated with light having coherence that is a known function of r, the distance along that plane from the optical axis. We will now discuss some details of the experimental arrangement for the holographic measurement of this coherence.

The object O and the aperture for the reference beam are shown in detail in Fig 4-2. The object is a 1.4 X 1.8 inch piece of ground glass with radial lines marked in cm and originating at a point Q (at r = 0) where the optical axis intersects the plane of the object. Centered at r = 0 is a circular aperture of 2 mm radius. This is used to transmit the reference beam.

The analysis in Chapter 3 requires a highly coherent reference beam. Since the coherence of the light reaching the plane of the object varies with r as shown in Fig. 4-3, we see that the coherence of the light passed by the 2 mm aperture at Q has $|\gamma| \geq 0.97$ and provides a highly

coherent beam, since the common criterion for coherence in optics is $|\gamma| \geq 0.88$.

The reference beam thus produced is spread by passing it through a 3 cm focal length lens so that it illuminates a circle of about 15 mm diameter at the hologram plane, as indicated in Fig. 4-1. The focal point of this lens is the effective "point reference source" R in Fig. 4-1. Since it lies about 3 cm away from the plane of the object, the resulting hologram is not precisely a Fourier transform hologram (see Section 3.2). This manifests itself in the reconstruction by producing a mirror image in a plane slightly removed from the principal image plane.

The hologram is formed by interference between the reference beam and the light transmitted by the ground glass object. It is recorded on film positioned approximately 30 cm from the plane of the object.

A photograph of the system used is shown in Fig. 4-4. The components are mounted on a 2 meter optical bench and are identified with those in the schematic of Fig. 4-1. The black wooden box that appears at the right of the photograph is part of the enclosure that

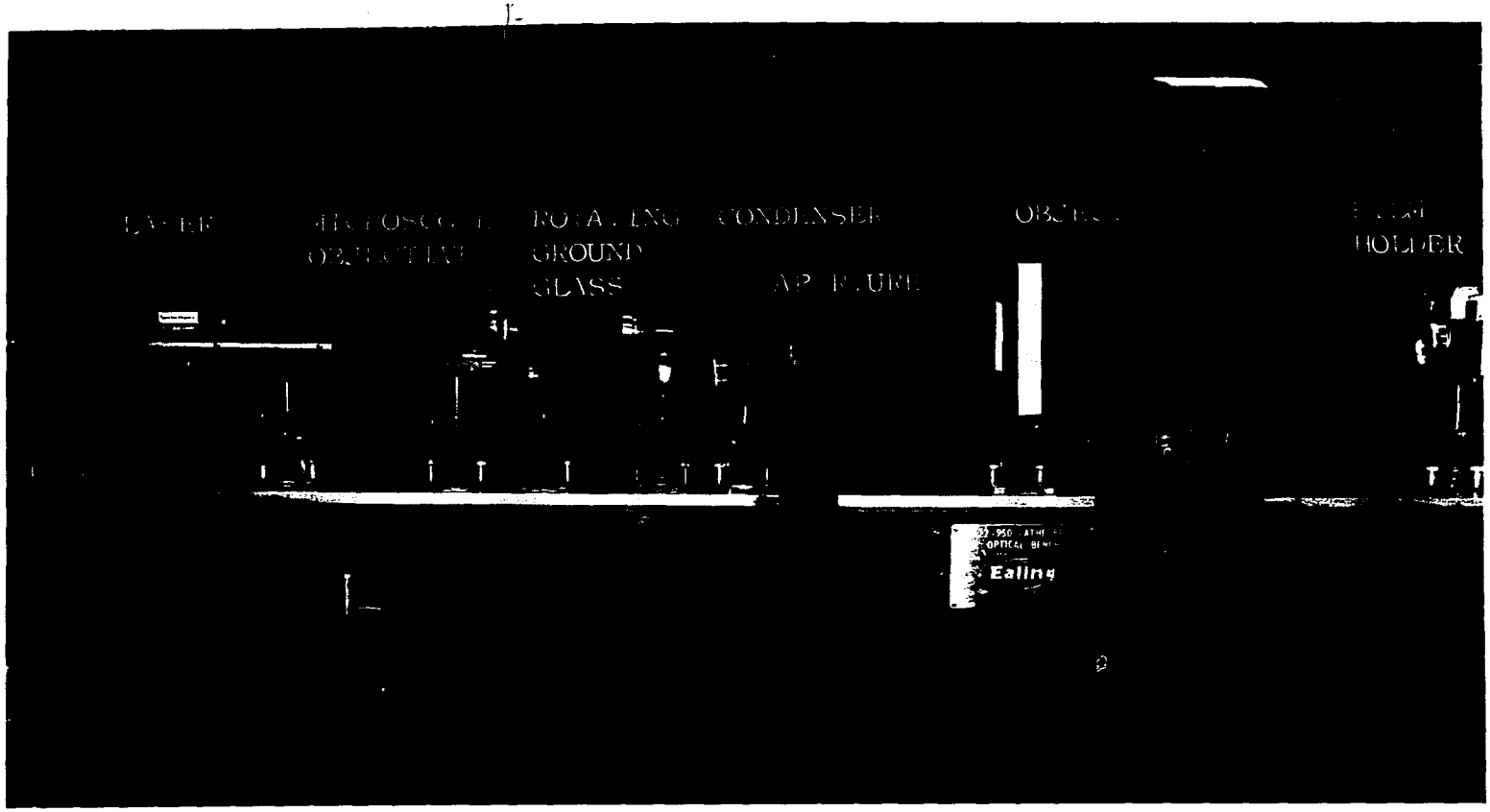

Figure 4-4. The system used to take holograms with partially coherent light.

prevents stray light from reaching the hologram apparatus during the exposure. Figure 4-5 is a close-up of the portion of the optics used to produce the partially coherent light. At the extreme right is a micrometer stand holding the small aperture A that illuminates the object plane with partially coherent light.

The object and the 2 mm aperture for the reference beam are held in the Al frame which appears quite bright in Fig. 4-4. The film for recording the hologram is held in the standard 35 mm camera back (no lens) shown.

Although the optical bench is of heavy iron construction, dimensional stability and vibration proved to be severe problems. Of course, these are the banes of all holographers for several reasons. The hologram consists of such a fine fringe pattern that motion of the film easily destroys the recording. Furthermore, it is apparent from Chapter 3 that any relative motion of the optical components (e.g. because of vibration or distortion of the bench due to temperature or stress) would change the optical path length between the various components, thereby varying the phase of the light reaching those components and reducing the coherence. (This

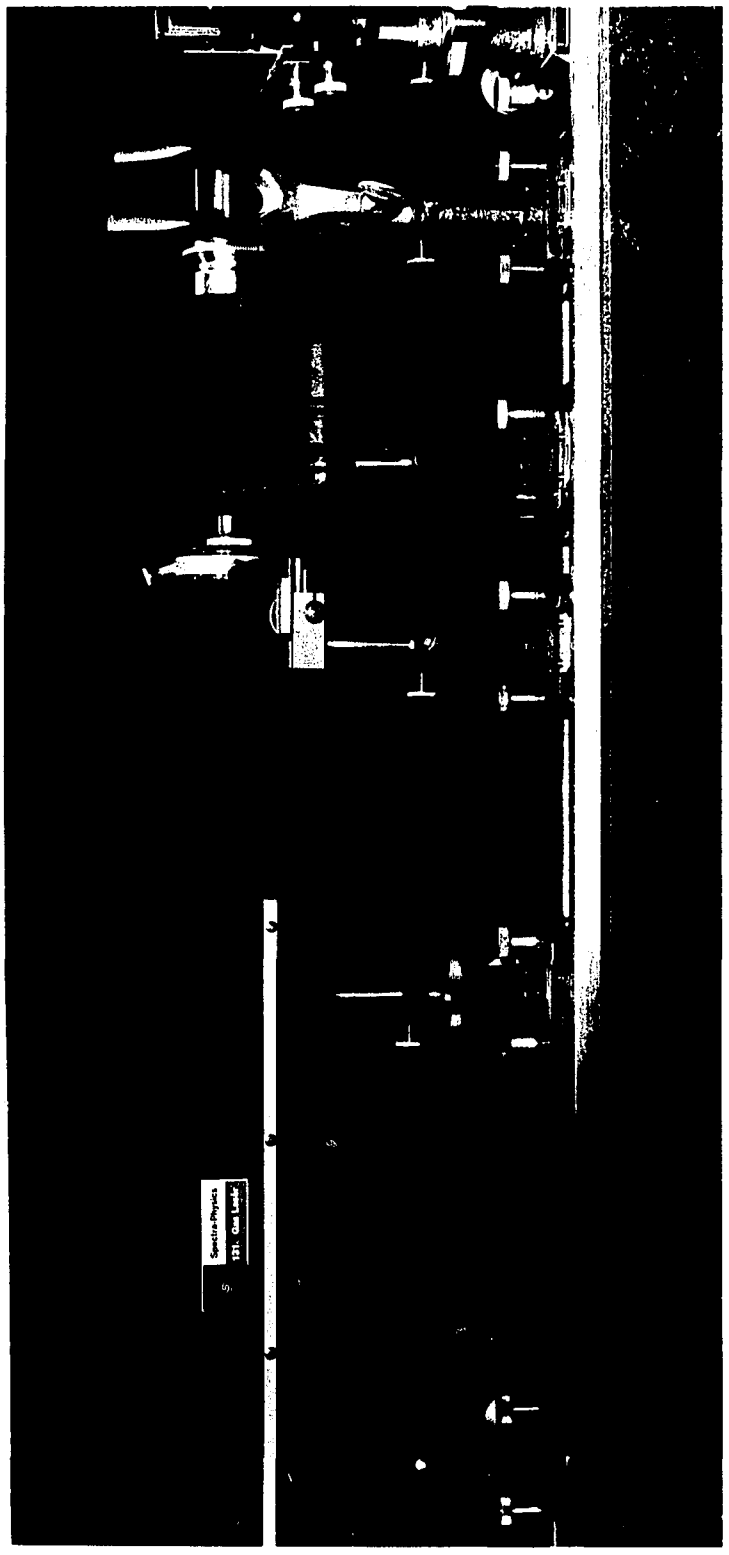

Figure 4-5. A close-up of part of Fig. 4-4. See text.

is discussed in detail in Chapter 5.) The magnitude of the difficulties encountered becomes apparent when one realizes that the stability of the components must be measured in fractions of the wavelength of the radiation used (6328 AU = 632.8 nm) during the entire exposure period which, for the holograms discussed here, was as long as six hours. Several minutes is a much more typical hologram exposure time, but the very small laser used in these experiments, plus the large light losses incurred in destroying and partially restoring the coherence account for the very long exposures.

As shown in Fig. 4-6, the entire table supporting the system was "floated" on four small inner tubes (6" Go-Kart tubes) inflated to about 5 psi each. This effectively decoupled the bench from vibrations in the building. To reduce air currents and thermal changes, exposures were started by a timer about an hour after the windows and doors to the laboratory were closed. The timer also stopped the exposures. Furthermore, the unusual six hour exposures were made in the middle of the night while there was little activity in the building.

To minimize the detrimental effects of the remain-

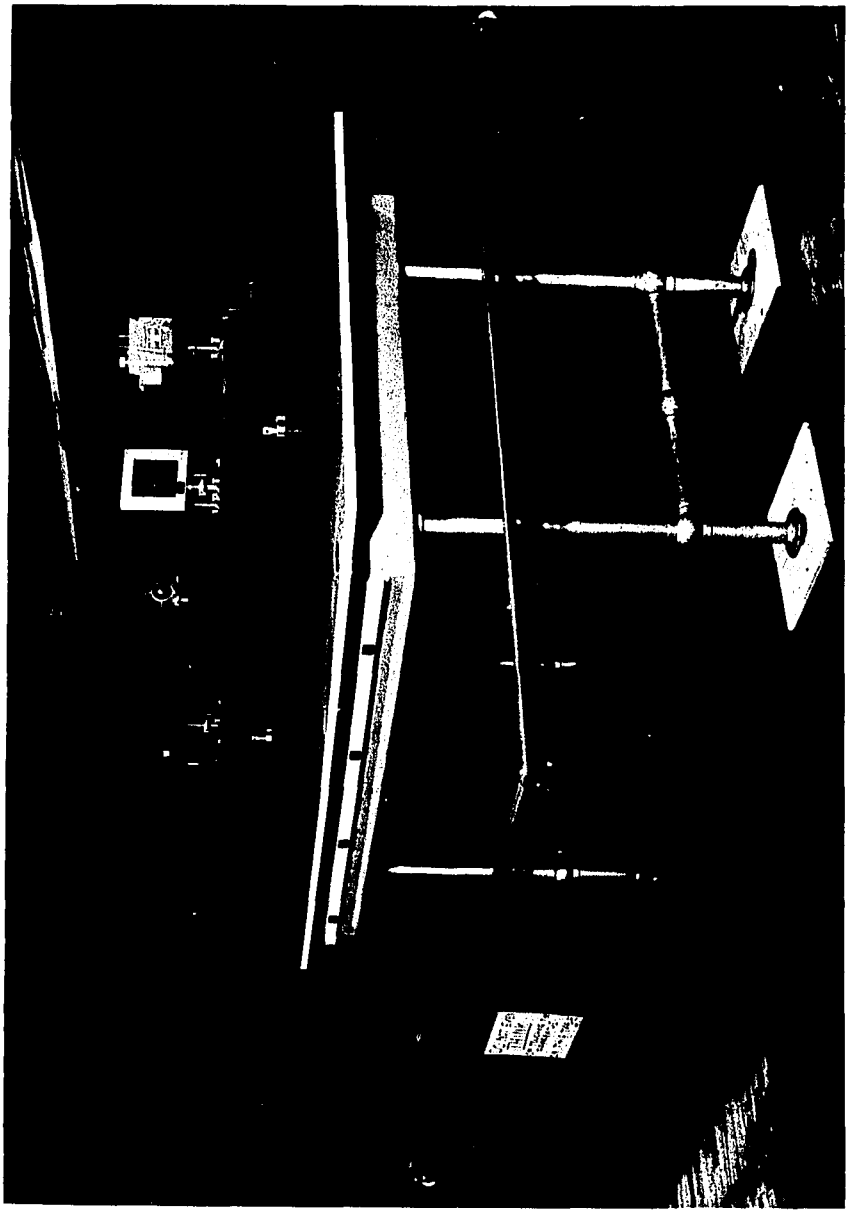

Figure 4-6. A view of the complete hologram system.

ing mechanical instability, the separation between the reference beam and the object was kept small, producing interference fringes with relatively wide spacing. This reduced the upper spatial frequency limit of the hologram resolution, but was not a problem here since no fine detail had to be resolved. Figure 4-7 is a top view of the object, aperture and lens for the reference beam, and the film. The largest angle of intersection, β, between the beams will be produced by the point m farthest from the reference source R and will occur at the point on the film located along the perpendicular bisector of the line segment Rm. The ratio of the distances S/D is much larger in the apparatus than in the figure; for large S/D the perpendicular bisectors of the two line segments Rm and Qm nearly coincide. Therefore, the angle β can be approximated using the geometry shown in the figure. For S = 300 mm, D = 50 mm, the resulting maximum fringe rate is approximately 270 cycles/mm (dark and light fringes/mm).

The lower fringe rate clearly reduces the harm done by a small movement of the film during exposure; and it permits the use of faster film with lower resolution.

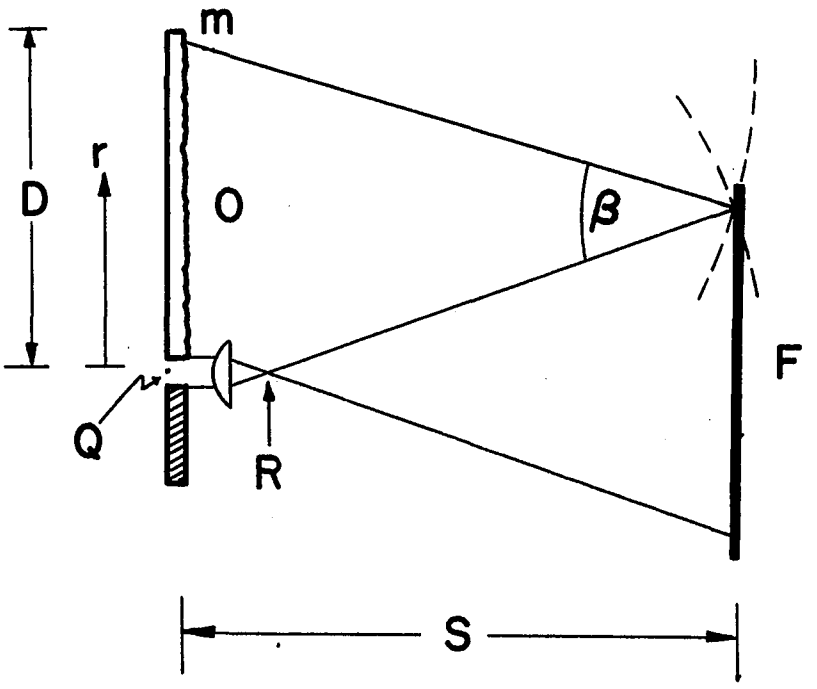

Figure 4-7. Top view of the ground glass object O, the small circular aperture centered at Q (at r = 0) which transmits the reference beam, the lens that spreads the reference beam and the film F that records the hologram. The dashed lines indicate the two interfering wavefronts. R is the effective position of the reference source.

For comparison, note that the hologram from which the reconstructions of Fig. 1-3 were made contains fringe rates as high as 1600 cycles/mm and was recorded on very slow Kodak 649-F plates. Kodak 35 mm size Hi. Def. Aero Type SO-243 film was used for the holograms being discussed in this section. This is a film available on special order, and is about four times more sensitive than 649-F plates with a corresponding lower resolution. Before Type SO-243 was recommended by the manufacturer, Kodak High Contrast Copy film was used. This is perhaps the only film (with the exception of Polaroid P/N) regularly stocked by photography stores on which reasonably good holograms can be recorded. However, because its resolution of 225 cycles/mm is barely acceptable, and its long wavelength response starts to fall off before 6328 AU, Type SO-243 was more suitable.

4.3. Measurement of Spatial Coherence by Means of a Hologram

In Chapter 3 we showed that the distribution of irradiance in a reconstructed real image was proportional to the square of the magnitude of the coherence of the illumination (during the exposure) at each point of the

object, measured with respect to the reference beam. Therefore, by measuring this irradiance, the variation of $|\gamma|^2$ over the surface of the object could be determined. In the example considered here, of course, we expect $|\gamma|$ to vary as predicted in Fig. 4-3.

To show this, a hologram was taken with the system described in the previous section, and a real image was reconstructed by the method of Section 3.2.2.

Figure 4-8a is a conventional "snapshot" of the object illuminated with the partially coherent light reaching it from the aperture A. The characteristics of the snapshot are independent of coherence and show the object as it appeared to the eye. Figure 4-8b is a reconstruction of the hologram made of the object illuminated precisely as it was when the snapshot was taken. The reconstruction was made by simply exposing a sheet of Polaroid P/N film in the plane of the real image. The expected shading with distance from the point Q centered at $r = 0$ is apparent and corresponds to the predicted variation of coherence. The overexposed central spot (hot spot) around the optical axis is due to the portion of the bright reconstructing beam that passes straight

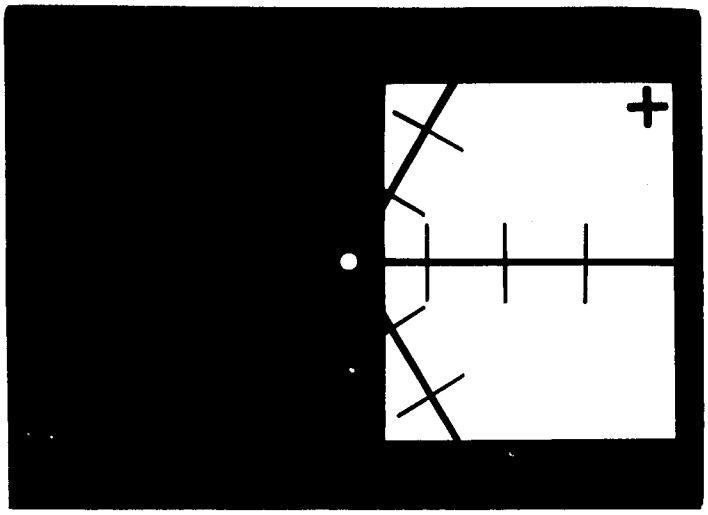

Figure 4-8a. A conventional snapshot of an object illuminated with partially coherent light.

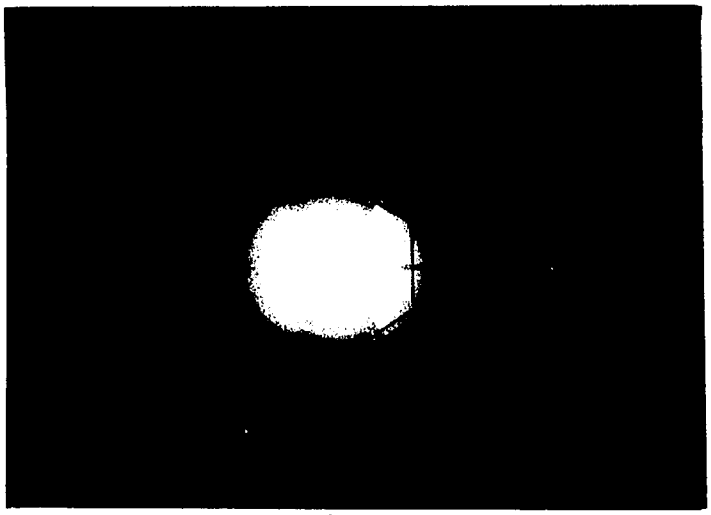

b. A hologram reconstruction of the same object.

through the hologram. The image of the ground glass with the radial markings can be seen. The positions of the first dark ring and first bright ring are in good agreement with the first zero and second maximum of the coherence (r = 14.9 and r = 20.0 mm, respectively) in Fig. 4-3.

The magnitude of the degree of coherence was measured quantitatively by measuring the irradiance at the real image plane as a function of r, where r is defined as in the previous sections. The measurements were made with an 0.5 mm diameter aperture mounted in front of a photomultiplier tube. The aperture and tube were moved in steps of about 1 mm along a radial line through the point at r = 0. The measured values of irradiance agree well with the distribution of coherence calculated in Section 4.1 except in regions of low coherence. The low image irradiances corresponding to low coherence were masked by the relatively high level of background light. There seem to be two reasonable causes of this background. First, the relatively fast film used consists of large grains which scatter a large portion of the incident light. Second, the two terms in the reconstructed wave that we have been ignoring throughout our calculations

represent additional light. For the real image reconstructed by a Fourier transform hologram, Eqn. 3-23 shows that these terms are

$$A(P)\left[\langle I_o(P)\rangle + \langle I_R(P)\rangle\right]\cos\left(\omega(t + s_{PF}/c)\right) \quad .$$

The light associated with this expression is independent of the real image; it therefore represents background or noise. A detailed study of this radiation would seem to be a useful extension of the present calculation.

In spite of these difficulties, the second maximum in the coherence was detectable, yielding a measured value of $|\gamma| = 0.12$ compared to the calculated value of $|\gamma| = 0.132$. For larger values of $|\gamma|$ the agreement improved.

The measured irradiances at various distances from the point Q at r = 0 are given in Table 4-1, and are plotted in Fig. 4-9 with the theoretical dependence of $|\gamma|^2$ on r shown for comparison. The agreement is very good except as discussed above. The minimum at r = 14.9 mm and the second maximum at r = 20.0 mm were clearly detectable in the photograph in Fig. 4-8b, although the minimum is not evident in the photomultiplier readings. Since the coherence could not be measured at r = 0

TABLE 4-1

Radial distance along real image plane from optical axis	Irradiance at real image plane	
r (mm)	I (arbitrary units)	$\lvert\gamma_r(0)\rvert^2$ †
5.85	11.0	.55
6.25	10.1	.51
6.5	9.76	.49
7.0	8.80	.44
7.5	7.46	.37
8.0	6.27	.31
8.5	5.36	.27
9.0	4.40	.22
9.5	3.49	.17
10.5	2.1	.11
11.5	1.26	.063
12.0	1.10	.055
13.0	.69	.035
14.0	.41	.021
15.0	.30	.015
16.0	.24	.012
17.0	.24	.012
18.0	.26	.013
19.0	.26	.013
20.0	.28	.014
21.0	.27	.013

†Adjusted to agree with theoretical value at r = 5.85mm.

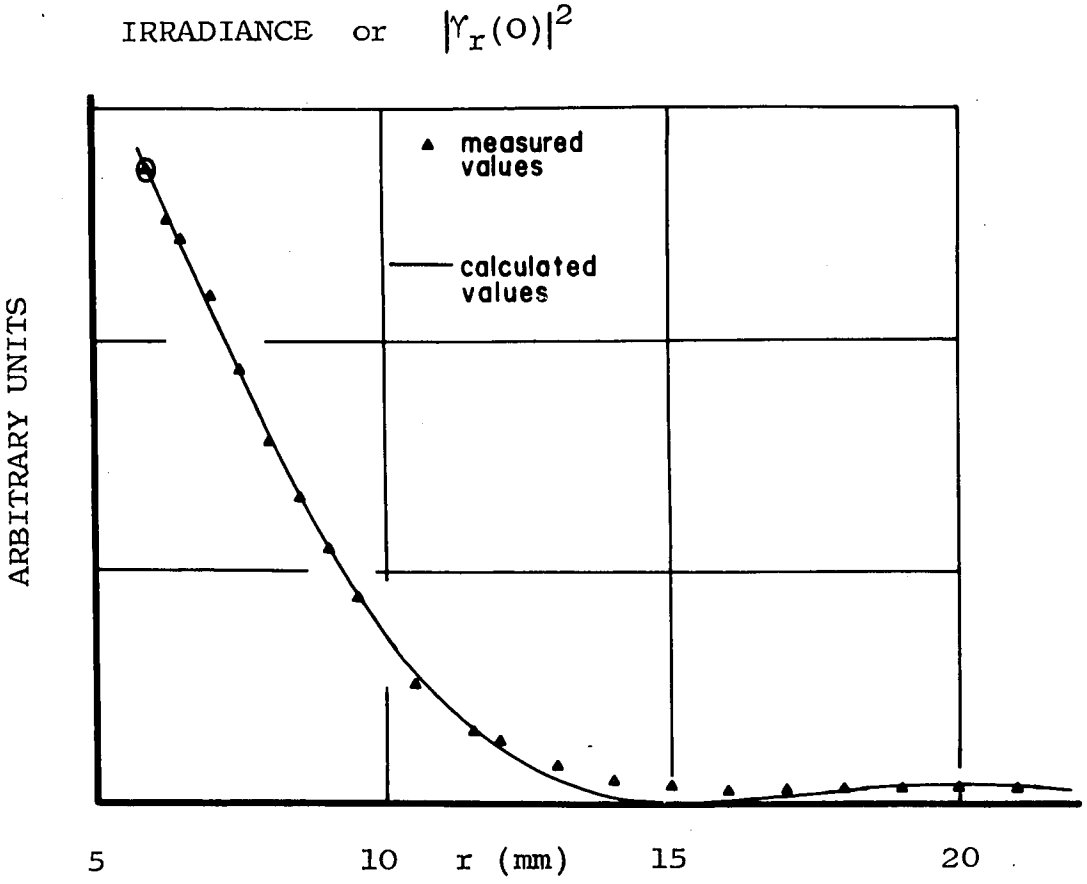

Figure 4-9. An example of holographic measurement of spatial coherence, showing the agreement with calculated values. The magnitude of the curve was fitted to the data at the circled point. The second maximum at r = 20.0 mm is detectable in the original data.

because that point is in line with the bright reconstructing beam, the magnitude of the theoretical curve had to be fitted to the data at a different point, indicated in the figure and in the table.

It seems apparent that this method could be used to measure the spatial coherence of any q-m light source if sufficient light, or an adequate emulsion, were available.

CHAPTER V

APPLICATION OF HOLOGRAPHY TO THE MEASUREMENT OF VERY SMALL MOTIONS[1]

We have seen in Chapter 4 how holography can be used to measure spatial coherence. We will now show that this leads to a very sensitive technique for measuring small displacements or velocities.

5.1 Analysis of the Coherence of Radiation Reflected from a Moving Object

Consider coherent radiation incident on a diffusely reflecting object. If the object moves, the relative phase between the incident and reflected radiation at a given point varies as a function of time, so that the coherence between these two beams is reduced. A hologram produced by using the reflected radiation as the object beam, and part of the incident radiation as a reference beam, would display this variation of coherence and would, therefore, indicate the motion of the object. We want to calculate the coherence between a beam directed towards an element m of some object, and the beam reflected from m towards a point P. The calculation will be carried out

at the position of m at t = o, as in Fig. 5-1. Both the phase φ and the frequency ω of the radiation reflected by the moving element m will vary with time, the latter due to the Doppler shift. Although one is tempted to neglect the Doppler shift because of the very small velocities being considered, we will show that the effect is appreciable.

This is not strictly a coherence problem, since the variations in ω and φ may be not only random or periodic, in which cases our definition of coherence, Eqn. 2-3, is meaningful[2], but may be any arbitrary function of time. For example, for any object displacement that is a monotonic function of time, the coherence Υ defined by Eqn. 2-3 approaches zero for large T, because the frequency of the reflected radiation will then be consistently greater or smaller than the frequency of the incident radiation. However, the integral implied by Υ_{Rm} in Eqns. 3-4 and 3-15, which later affects the reconstructed image, is not rigorously a time average (i. e. an integral as T approaches infinity), but is an integral over the exposure time T which is finite. Rigorously, we should not call this coherence here, but, no matter what we call it, this is

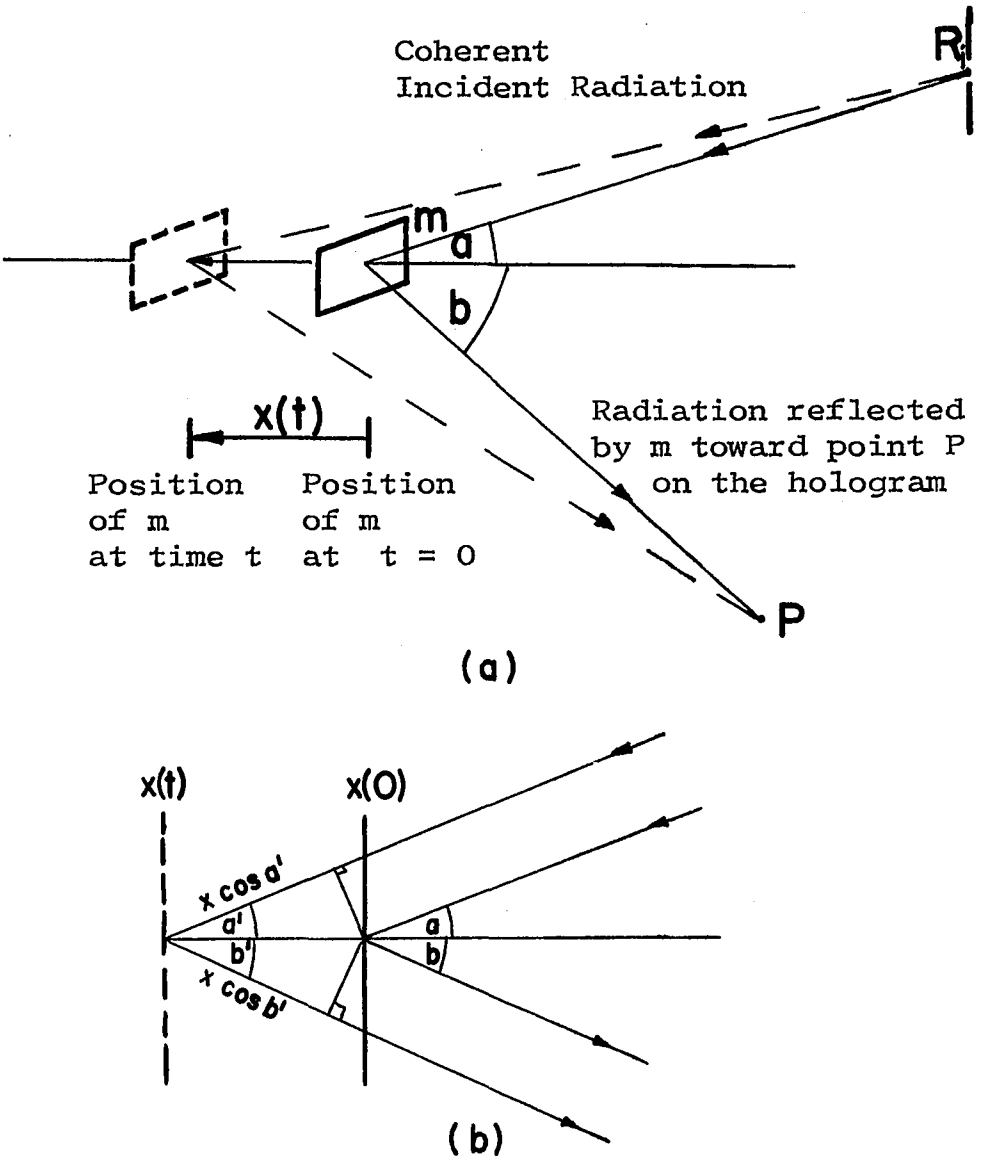

Figure 5-1. The geometry for calculating the loss of "coherence" when coherent radiation is reflected from a moving object.

the integral that affects the reconstructed image.

From Eqn. 3-11 for a plane wave reference beam, we see that the reconstructed wave depends on the "coherence" through the term $|\gamma_{Rm}(\tau_{mRP})|$ or, for q-m radiation, through the term $|\gamma_{Rm}(0)|$. For the sake of precision, let us call this term $|g_{Rm}(0)|$ here, to indicate that it is similar, but not identical, to coherence. Then

$$g_{Rm}(0) = \frac{\frac{1}{T}\int_0^T V_R(t)\, V_m^*(t)\, dt}{\left[\langle I(R) \rangle \langle I(m) \rangle \right]^{\frac{1}{2}}} \qquad (5\text{-}1)$$

where T is the exposure time of the hologram. Here, $V_R(t)$ is the analytic signal at the source of the reference beam and $V_m(t)$ is the analytic signal produced at the initial position of m (x = x(0) in Fig. 5-1a) due to the radiation reflected from the displaced m. Therefore, both the frequency and the phase of $V_m(t)$ may vary with time. We will justify the continued use of the q-m approximation later; for now we assume that the Doppler shift is small enough to permit this.

If $V_R(t)$ and $V_m(t)$ have constant amplitudes A_R and A_m, conditions that are easily maintained experimentally, we can write

$$V_R(t) = A_R e^{j\omega t}$$

$$V_m(t) = A_m e^{j\left[\int_0^t \omega'(t')dt' + \phi_m(t)\right]}$$

$$I(R) = A_R^2$$

$$I(m) = A_m^2 \quad .$$

If we write

$$V_R(t) = A_R e^{j\int_0^t \omega\, dt'}$$

then Eqn. 5-1 simplifies to

$$q_{Rm}(0) = \frac{1}{T}\int_0^T e^{-j\left[\int_0^t (\omega'(t')-\omega)\,dt' + \phi_m(t)\right]} dt \quad . \tag{5-2}$$

As long as the q-m approximation is valid, the arguments of Chapter 3 apply and the brightness of the point in the reconstruction corresponding to m is proportional to the squared magnitude of the integral in Eqn. 5-2.

Before we investigate this integral, we must demonstrate that the q-m approximation is valid in view of the

Doppler shift produced by the moving object. It may be helpful to visualize a particular arrangement for producing the hologram as shown in Fig. 5-2. When radiation of frequency ω is reflected from the object receding with the velocity v, the frequency of the reflected radiation is[3]

$$\omega'(t) = \omega\left(1 - \frac{v(t)}{c}\right) \qquad (5\text{-}3)$$

where c is the velocity of the radiation, here the velocity of light. The q-m condition is satisfied if

$$\tau \ll 2\pi/\Delta\omega$$

where τ is defined according to Eqn. 2-4 as

$$\tau = \Delta s/c$$

Here Δs is the greatest difference between the optical path lengths traveled by the reference and object beams. Referring to Fig. 5-2,

$$\Delta s = \left|\begin{array}{l}\text{optical path length from laser to stationary} \\ \text{mirror to hologram - optical path length} \\ \text{from laser to object to hologram}\end{array}\right|_{max}$$

From Eqn. 5-3,

$$\Delta\omega = \omega'(t) - \omega = \omega\frac{v(t)}{c} \qquad (5\text{-}4)$$

A little manipulation yields

$$\Delta s \ll c\,\frac{\lambda}{v(t)}$$

Since, for the experiments that will be discussed here,

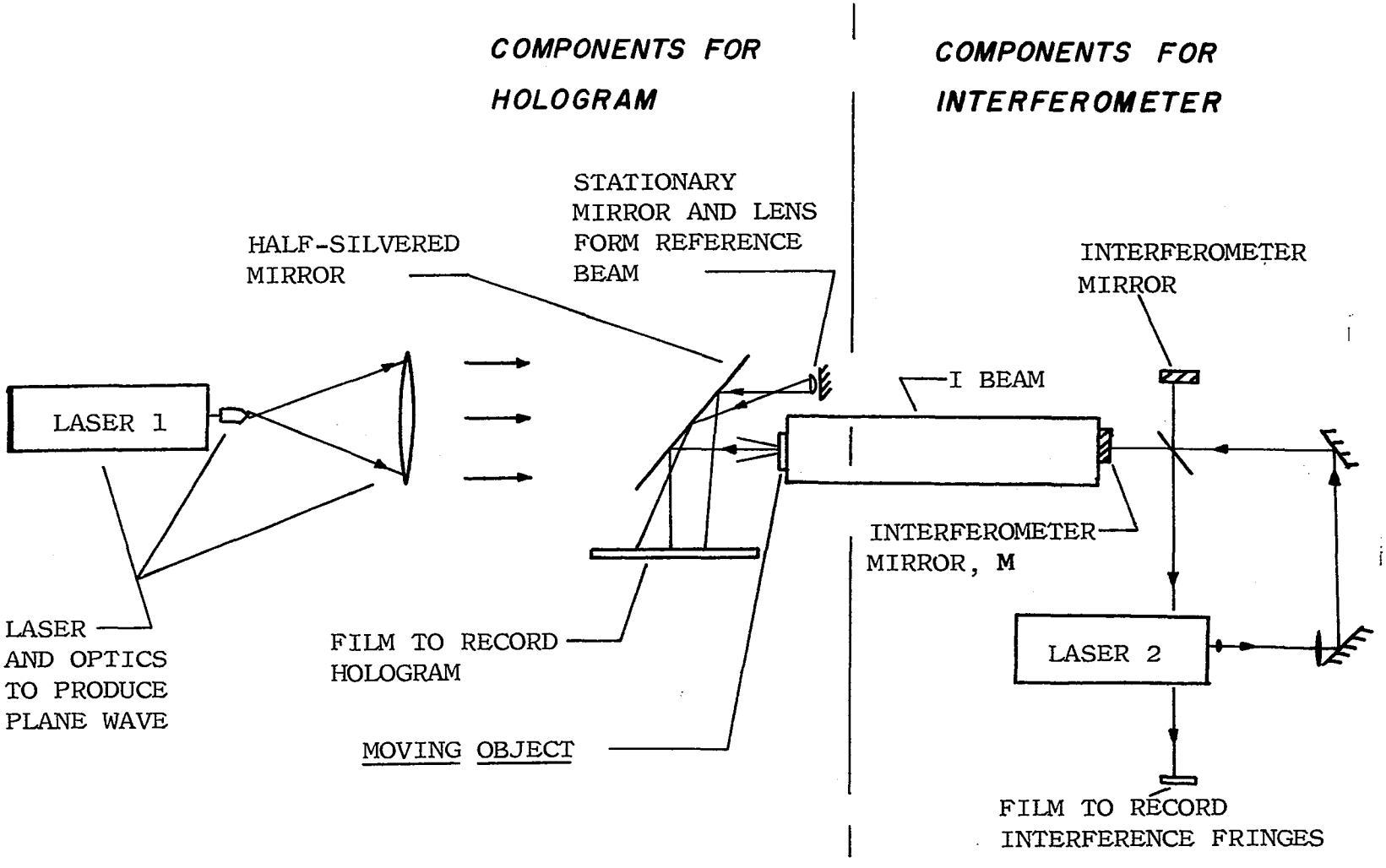

Figure 5-2. Top view of apparatus for taking a hologram of a moving object.

v will always be less than a wavelength per second, we require only

$$\Delta s \ll 10^{8} \text{ meters} \quad .$$

Generally, Δs is of the order of centimeters so the q-m approximation is unaffected by the Doppler shift. In fact, Δs is limited by the laser coherence length which is about 50 cm. for the laser used in this work.

Now let us investigate the integral in Eqn. 5-2 for an object point m moving with a displacement that is an arbitrary function of time, x(t). The geometry of the problem is shown in Fig. 5-1a. Since we expect this technique to detect motions of the order of wavelengths of light, it is reasonable to assume that the maximum value of the displacement x(t) will be much less than the distances from P to m and from P to the illuminating source R_i. With this approximation we can say

angle a = angle a' and angle b = angle b'

in Fig. 5-1b. Notice that for plane wave illumination of the object as in Fig. 5-2, R_i is at infinity. At time t, the element m has moved from x(0) = 0 to x(t). According to Fig. 5-1b, the radiation then travels an additional distance x(t)cosa before reflection and x(t)cosb after

reflection. Therefore, the total change in the phase of the radiation from m is

$$\varphi(t) = -\frac{1}{c}(\omega \cos a + \omega'(t) \cos b)\, x(t) \quad .$$

Since $\omega'(t) = \omega(1 - \frac{v(t)}{c}) \cong \omega$, we can approximate

$$\varphi(t) = \frac{-\omega}{c}(\cos a + \cos b)x(t) \qquad (5\text{-}5)$$

for $v \ll c$. The change in frequency is given by

$$\omega'(t) - \omega = -\frac{\omega}{c}\, v(t) \quad .$$

Therefore, the integral (5-2) becomes

$$g_{Rm}(0) = \frac{1}{T}\int_0^T e^{j\left[\frac{\omega}{c}\int_0^t v(t')dt' + \frac{\omega}{c}(\cos a + \cos b)\, x(t)\right]} dt \qquad (5\text{-}6)$$

$$= \frac{1}{T}\int_0^T e^{j\frac{\omega}{c}\left[1 + \cos a + \cos b\right]x(t)}\, dt$$

where T is the hologram exposure time.

g_{Rm} cannot be simplified further without knowing something of x(t) and the angles a and b. If a and b are small, we can immediately write

$$g_{Rm}(0) = \frac{1}{T}\int_0^T e^{j\frac{\omega}{c}(3)x(t)}\, dt = \frac{1}{T}\int_0^T e^{j\frac{6\pi}{\lambda}x(t)}\, dt. \qquad (5\text{-}7)$$

With the arrangement illustrated in Fig. 5-2, angles a and b are both zero and this result is exact. To calculate

the appearance of a reconstruction of a hologram of a moving object subject to the conditions that the hologram was made with q-m light and a plane wave reference beam, we must evaluate the integral in Eqn. 5-7 and substitute the resulting value of $|g_{Rm}|$ into Eqn. 3-11 in place of $|\gamma_{Rm}|$.

The preceding discussion is easily generalized to include reference beams that are not plane waves by simply replacing $V_R(t) = A_R\, e^{j\omega t}$, which represents the reference beam, by $A_R\, e^{j(\omega t + \theta_p)}$, where θ_p is an arbitrary function of position independent of time, but dependent on the shape of the wavefronts. This constant phase then appears in each following equation, finally adding a constant phase to g_{Rm} in Eqn. 5-7. Since the reconstruction depends on $|g_{Rm}(0)|$, this phase has no effect. This result is significant because holograms are often most easily made with spherical wave reference beams as discussed in Sect. 3.2.

5.2. Holographic Measurement of the Displacement of an Object Moving with Approximately Constant Velocity

The integral in Eqn. 5-7 is easily evaluated for constant velocity v(t). Therefore, measuring the displacement of an object moving with a very small, constant velocity seemed to be a worthwhile demonstration of a possible application of the analysis above. To make the experiment more meaningful, it seemed desirable to measure the same displacement by another independent method. Unfortunately (or, perhaps, fortunately), holography appears to be more sensitive than other available techniques. Nonetheless, a standard Michelson interferometer[4] arrangement for measuring displacements was found to be sensitive enough to provide an approximate check on the holographic measurements. The theory, technique and results of these experiments are discussed next.

If $v(t) = v$, a constant velocity, then, since $x(t) = vt$, Eqn. 5-7 becomes

$$g_{Rm}(0) = \frac{1}{T}\int_0^T e^{j\frac{\omega}{c}(3vt)}\,dt = \frac{1}{T}\int_0^T e^{j\frac{6\pi}{\lambda}vt}\,dt \qquad (5\text{-}8)$$

$$= \frac{1}{6\pi j N(T)}\left[e^{6\pi j N(T)} - 1\right]$$

where N(T) (measured in number of wavelengths, i. e. $N(t) = x(t)/\lambda$) is the total displacement during the exposure time T. For N(T) = 0, $g_{Rm}(0) = 1$ as expected for a stationary object. From Eqn. 5-8, we find that

$$\left|g_{Rm}(0)\right|^2 = \frac{2 - 2\cos\beta}{\beta^2}$$

where $\beta = 6\pi N(T)$. The function is plotted in Fig. 5-3. Notice that the secondary maxima are given by

$$\left|g_{Rm}(0)\right|^2_{max} = \left[1/3\pi N(T)\right]^2$$

which lie on a curve asymptotic to the abscissa. The most striking aspect of Fig. 5-3 is that $\left|g_{Rm}(0)\right|^2$ has periodic zeros at $6\pi N(T) = 2\pi n$ or $N(T) = n/3$ or at $x(T) = n\lambda/3$. Therefore, a displacement of $\lambda/3$ would easily be detected by zero brightness in the reconstruction. Even more

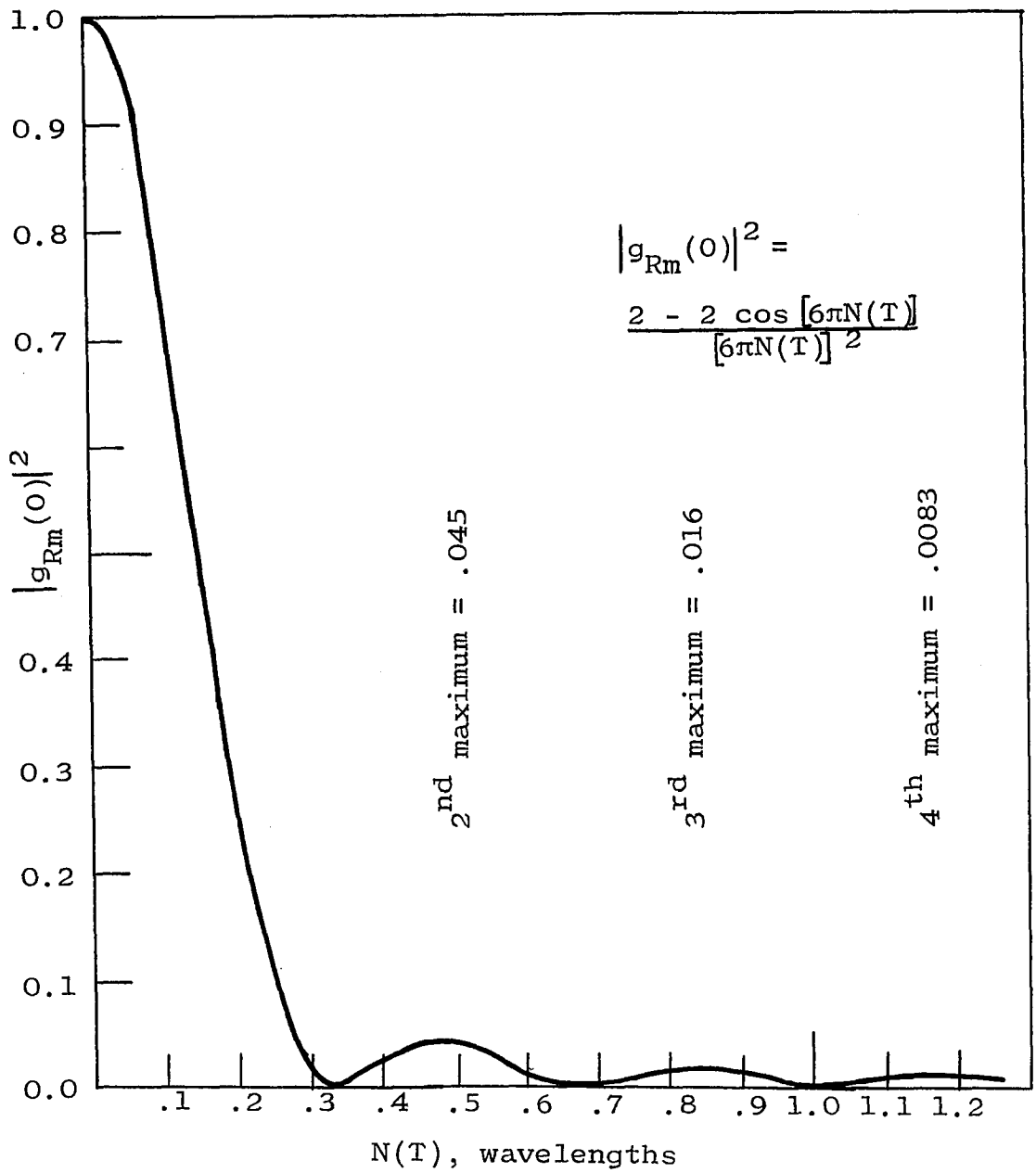

Figure 5-3. Graph showing the expected variation of $|g_{Rm}(0)|^2$ with displacement N(T) of an object moving with constant velocity. N(T) is measured in wavelengths of the radiation used.

interesting is the result that for larger displacements, corresponding to higher velocities during the exposure, the brightness in the reconstruction increases. It then falls off to a second zero and so on for increasing n.

The greatest practical problem in performing an experiment to measure a displacement of the order of $\lambda/3$ arose in producing this small displacement in a controlled way. The constant velocity v with which the object would have to move for the duration of the exposure time would be $v = x(T)/T$. Estimating exposure times at about one minute, we see that constant velocities of the order of 1/3 wavelength per minute are required.

Many approaches to this problem were tried and abandoned, each due to its own failures. These included piezoelectricity, mechanical demultiplication and compression under pressure (relaxation). Finally, thermal contraction was found to provide a satisfactory technique. An aluminum tube was first heated by means of two five watt resistors inserted within the tube, then allowed to cool to room temperature. The cooling and resulting contraction was, of course, exponential in time, but by controlling the thermal conductivity between the

heated tube and the surrounding ambient, the time constant could be made much longer than the exposure time, resulting in an almost linear motion during the time of interest.

Rather than measure the displacement of the end of the Al tube and obtain only one measurement for each hologram, the contracting rod was used to rotate a flat rectangular plate through a small angle, producing a range of velocities over the surface of the plate that varied with the distance from the axis of rotation. The possibility of measuring all these velocities simultaneously is an important advantage of this method over conventional interferometric techniques as explained later. The mechanical system is outlined in Fig. 5-4. A heavy I beam (to reduce vibration due to air currents and other disturbances) is supported at one end by the Al rod and at the other by a knife edge ground on the bottom of a piece of flat Al stock. The object that is holographed is a rectangular area 1" x 1.8" at the bottom of this flat piece that is covered with "Scotchlite" reflecting tape to increase the reflectance in the direction of the hologram plate, thereby decreasing the required exposure time.

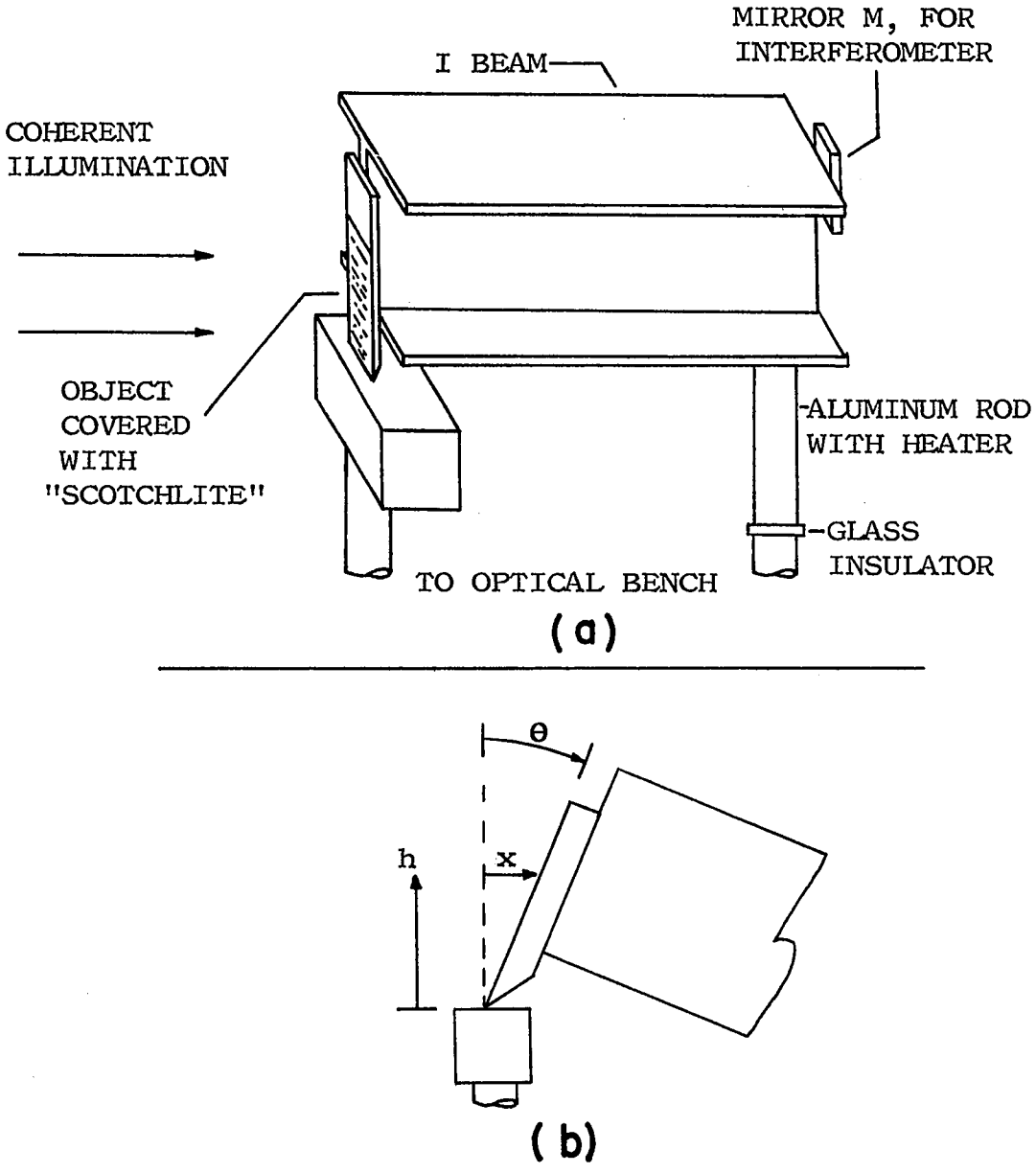

Figure 5-4. A drawing of the apparatus used to rotate an object through a very small angle θ by means of thermal contraction of an aluminum rod. In (b), θ is the angle of rotation of the object and d is the horizontal displacement of a point on the object located a distance h above the knife edge shown, so $x = h\theta$.

As the rod contracts, it is apparent that the object rotates away from the indicated illuminating beam. If the angle of rotation is θ as shown in Fig. 5-4b, then the displacement and velocity of any point a height h above the knife edge are, respectively,

$$x = h\theta \qquad \text{and} \qquad v = h\dot{\theta} \ .$$

A hologram reconstruction of such an object should be brightest at the knife edge where x and v are each zero, and should decrease to zero brightness at the height given by

$$x = h\theta = \lambda/3 \ . \tag{5-9}$$

For successively larger values of h, the brightness should increase then decrease periodically with decreasing maxima and with zeros at the heights for which $h = n\lambda/3\theta$. Thus, the object should appear brightest at the bottom and should show dark horizontal bands at the values of h given by the expression above. The dark bands should be more closely spaced for larger angular displacements θ.

The mirror M at the upper right of the I beam in Fig. 5-4 forms part of the Michelson interferometer which provides an independent, but less precise measure of the angle of rotation θ. This is a standard optical device,

used here mainly as an approximate check on the holographic results, and will not be analyzed here.[4] Briefly, this device was used in the following way. The fringe rate produced by the interferometer is a measure of the angle between the two interferometer mirrors, one of which is M. By photographing the fringes at known times while the object (and hence, mirror M) was rotating, it was possible to determine the change in the angle of the mirror M between these times. This change is equal to the angle θ through which the object rotated during the same time interval. The values of θ during several time intervals were fitted to an exponential curve, since the contraction of the cooling rod, and hence $\theta(t)$, are exponential functions of time. $\theta(T)$, the angular displacement during the exposure time T, could then be determined from the curve.

Figure 5-5 is a photograph of the apparatus. Because of the compactness and complexity of the system, the photograph is not as clear as we would like. However, certain essential features can be seen. The large I beam, just left of center in the photograph, is supported at the left by a bright Al bar, shaped to a knife edge and resting on a gray steel platform. The lower portion of

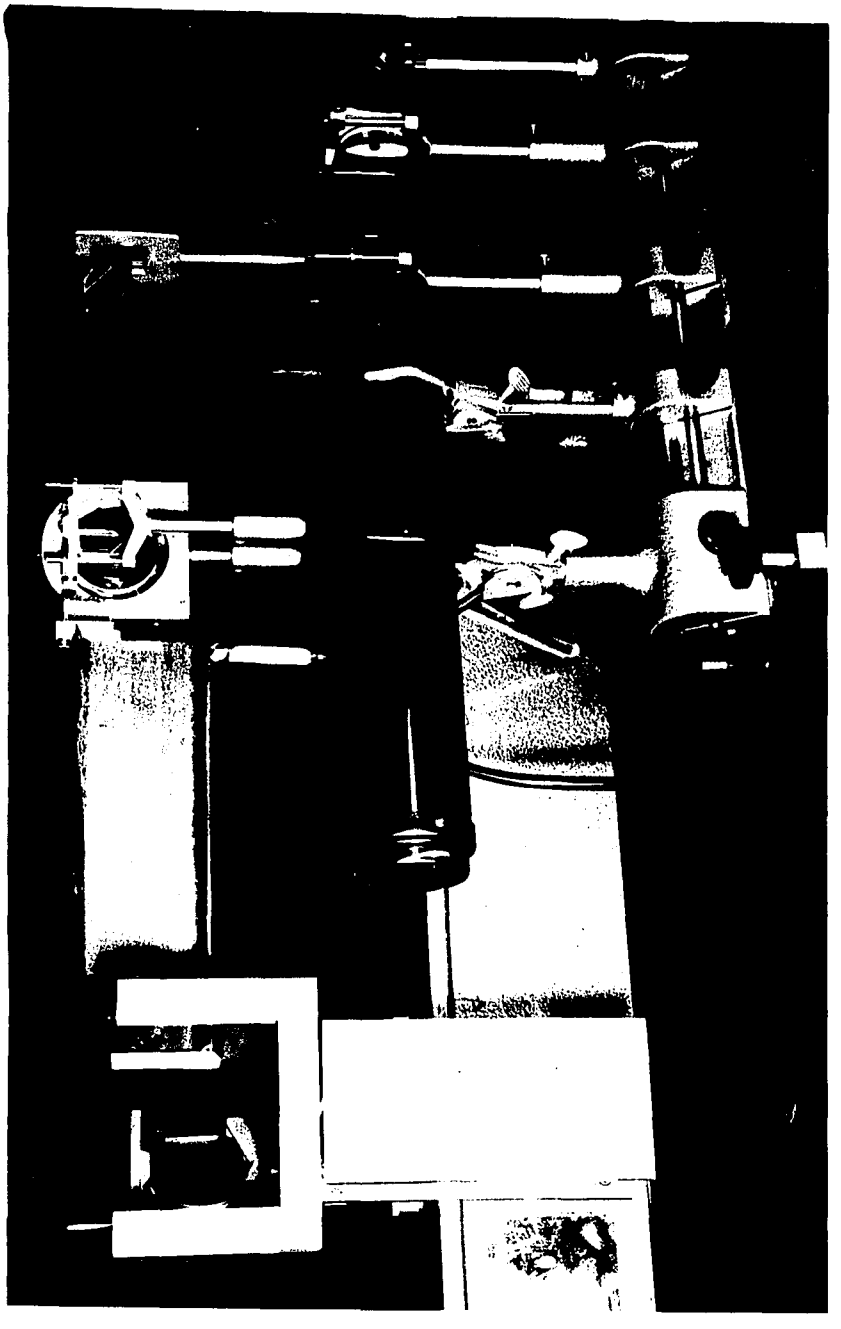

Figure 5-5. Apparatus used in moving object measurement.

the Al bar is the object that will be holographed. The I beam is supported at the right by a glass sphere (marble) attached to the vertical Al rod. The heater leads can be seen at the two ends of the rod.

The apparatus can be visualized best by considering the photograph in Fig. 5-5 and the top view drawing in Fig. 5-2. Everything pertaining to the hologram is left of the I beam while everything right of the I beam pertains to the Michelson interferometer. The laser beam (not seen in the photograph) used to take the hologram enters from the left, is reflected by the object and by a stationary mirror (not seen in the photograph) near the object, producing a reference beam. The object and reference beams are reflected by a semi-transparent mirror just left of the object onto a photographic plate that would be held in the bright U-shaped support in the foreground of Fig. 5-5. At the upper right of the I beam is the mirror labeled M in Fig. 5-2. The rather complicated looking pieces to the right of this are the other interferometer components. The light for this interferometer comes from a second laser (large black tube) and optics mounted on the small optical bench in the right foreground of the

photograph and is directed into the interferometer by the two round mirrors at the lower right and upper right of the photograph. This laser and associated optics are independent of the laser used to take the hologram.

Full size reconstructions of the real images of four holograms of the 1" x 1.8" rectangular object described above are shown in Fig. 5-6. They are arranged in order of increasing displacement θ. The first, A, is a reconstruction of a stationary object ($\theta = 0$). The highly directional reflectance of the "Scotchlite" covering the object, combined with non-uniform illumination by the laser, caused the central bright spot that is apparent in the figure. Although this altered the relative brightness over the reconstruction, it could not change the position of the bands of zero brightness.

According to Eqn. 5-9, the displacement at the first dark band was $\lambda/3$ so, assuming constant velocity, the velocity was $\lambda/3T$. The angular displacement of the object is simply $\theta = \lambda/3h$. The holographically measured velocities and angular displacements are given in Table 5-1 where they are compared to the approximate interferometer measurements. The agreement is well within the error of

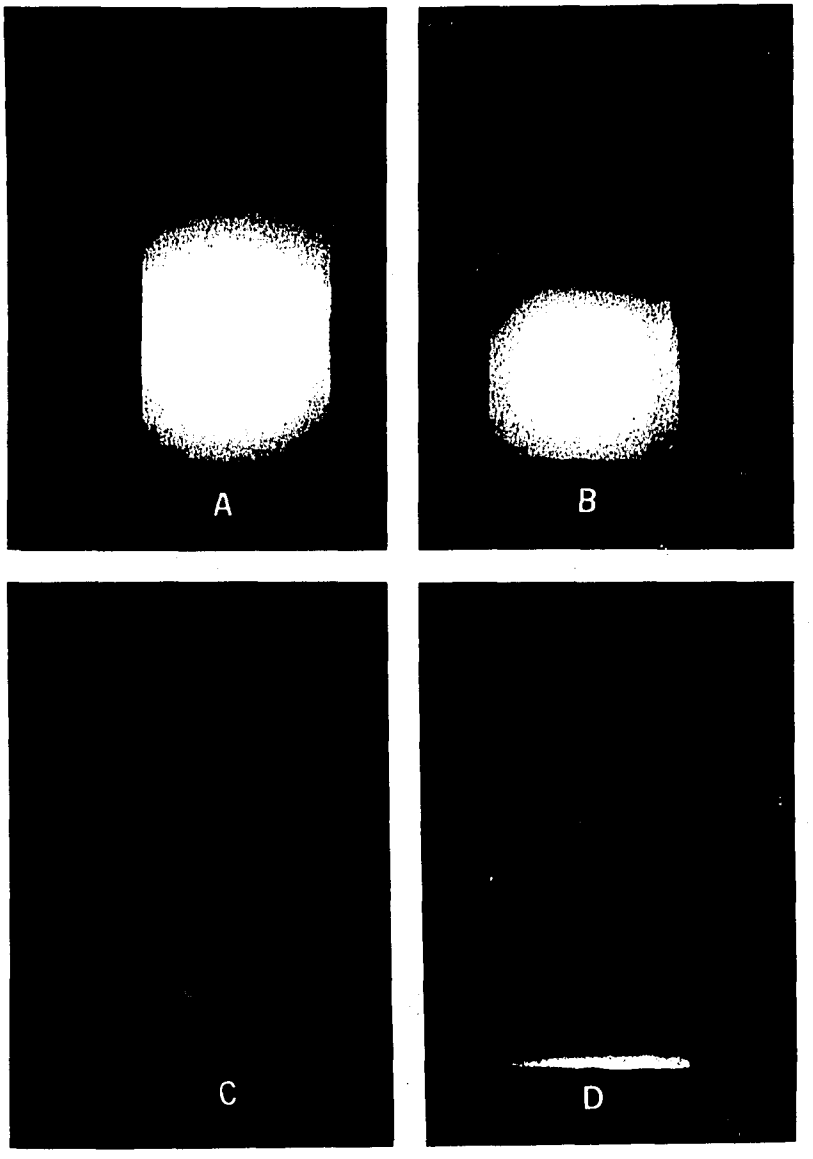

Figure 5-6. Reconstructions of moving objects. See text and Table 5-1.

TABLE 5-1

HOLOGRAM NUMBER	h AT FIRST DARK BAND	VELOCITY AT h BY HOLOGRAM	VELOCITY AT h BY INTERFEROMETER ±20%	θ BY HOLOGRAM	θ BY INTERFEROMETER ±20%
	mm	mm/sec	mm/sec	microradians	microradians
(a)	S T A T I O N A R Y				
(b)	30	7.0×10^{-6}	7.3×10^{-6}	7.0	7.3
(c)	16	7.0×10^{-6}	7.0×10^{-6}	13	13
(d)	3.2	1.4×10^{-6}	1.6×10^{-6}	66	75

the interferometer results which is estimated at ± 20%.

5.3. Additional Remarks on Holography of Moving Objects; Measurement of Sinusoidal Motion

Holography seems to offer several advantages over interferometry as a tool for measuring small displacements. The hologram technique is basically simpler, once one has a laser. The mechanical requirements are almost as severe in a precision interferometer as they are in a hologram system, and the interferometer requires more precision optical components and mechanical adjustments.

A further advantage of holography seems to be the ability to make measurements on ordinary (i. e. diffusing, curved, etc.) surfaces whereas an interferometer can measure the displacement of a high quality mirror of known shape (usually flat) only. In many situations, there is no convenient way to attach a mirror to the object whose motion is to be measured.

Perhaps the most important advantage of holographic measurement arises in the study of the class of measurement problems in which the motion of the object is complex or even non-rigid. In that case, the usual interferometric

technique of attaching a mirror or putting an optical finish on the object would not permit accurate measurement except with special precautions that effectively limit each measurement to only one point. The holographic technique measures the motion of the entire surface of the object, point by point, regardless of the complexity of the motion, or even changes in the shape of the object.

Finally, it should be mentioned that any motion for which the integral in Eqns. 5-6 or 5-7 could be evaluated could be measured holographically. For instance, for sinusoidal motion,

$$x(t) = A \sin \theta(t)$$

so that Eqn. 5-7 for small angles a and b becomes

$$g_{Rm}(0) = \frac{1}{T}\int_0^T e^{i\frac{6\pi}{\lambda} A \sin \theta(t)}\, dt .$$

Comparing this with standard forms of the Bessel functions[5], we can show that for exposure times T much larger than $2\pi/\omega$, the period of oscillation of the object,

$$g_{Rm}(0) = J_o(6\pi A/\lambda) , \qquad (5\text{-}10)$$

showing that for sinusoidal motion, there will also be regions of zero brightness in the reconstruction which could be used to measure the amplitude of the motion of

the object.

Equation 5-10 is in general agreement with the results of Powell and Stetson,[6] who have published reconstructions of holograms of vibrating diaphragms. Those reconstructions show dark fringes that follow expected loci of points of equal vibration amplitude as predicted. They calculated an expression for the brightness of the reconstruction in a different way and obtained an expression that also depended on the Bessel function but in which the argument of J_o was $(4\pi A/\lambda)$. The difference is due to the inclusion of the Doppler effect in the calculation presented here. The change in the argument results in a different interpretation of the motion producing a given hologram, since the dark fringes corresponding to zeros of J_o will occur at different vibration amplitudes.

For more general forms of motion, the integral in Eqn. 5-6 might be evaluated numerically. In this way, the holographic technique could be applied to the measurement of almost any motion, provided the specific form of the motion is known.

REFERENCES

1. Portions of the work in this section have been presented to the Optical Society of America, 1967 Spring Meeting, April, 1967, Columbus, Ohio.
2. M. J. Beran and G. B. Parrent, Jr., Theory of Partial Coherence, Prentice Hall, N. J., 1964, p. 28.
3. F. A. Jenkins and H. E. White, Fundamentals of Optics, McGraw-Hill, N. Y., 1957, p. 204.
4. Ibid., p. 244.
5. E. Jahnke and G. Emde, Tables of Functions, Dover Publications, N. Y., 1945, p. 149.
6. R. L. Powell and K. A. Stetson, J.Opt.Soc.Am. 55, 1593 (1965).

CHAPTER VI

CONCLUSIONS AND RECOMMENDATIONS

We have shown that partially coherent light can be used to produce a clear, undistorted hologram provided that all the light reaching the hologram is quasi-monochromatic and the reference beam has a high degree of spatial coherence. The effect of the partial coherence of the illumination is only to make the reconstructed image darker. Furthermore, the light distribution in the reconstruction is proportional to the magnitude squared of the degree of coherence of the light illuminating the object during the production of the hologram.

The techniques developed in Chapter 4 show how the magnitude of the degree of coherence at each point over an entire surface can be directly obtained from a measurement of the irradiance at the real image reconstruction. By comparison, conventional interference techniques for the measurement of coherence by means of visibility require repeated observation for each and every point of interest on a surface. The hologram

technique instead provides a permanent record of the distribution of coherence over the whole surface. Furthermore, the required measurement of irradiance is simpler than the measurement of the visibility of an interference pattern.

A similar measurement of irradiance can be used to measure small displacements of an object, even if they occur over long periods of time. Such measurement is possible, however, only if one has a priori knowledge of the form of the relationship between displacement and time.

Several extensions of the fundamental research and the applications seem promising. The technique for measuring displacements discussed in Chapter 5 could be verified for more complex forms of motion by evaluating Eqn. 5-6 on a computer. To test this, a surface executing a known but complex motion could be provided by electrically exciting a piezoelectric element. After experimental verification, the technique could be applied to the study of motions that could not otherwise be measured. For example, holography could be used

to measure the electro-mechanical coupling (under actual operating conditions) of a transducer such as a microphone, hydrophone, accelerometer, etc. For many of these devices, a simple assumption of linearity might be acceptable in the a priori determination of the type of motion.

Improvement in the experimental techniques (e.g. by the use of a more powerful laser) could be fruitful. This could result in a more accurate verification of the theory and could extend the range and improve the precision of the practical applications. It could also permit detailed investigation of some inherent sources of inaccuracy in many holographic measurements.

An extension of this work to non-quasi-monochromatic light is also indicated. It seems reasonable that the characteristics of a reconstructed image would depend on temporal coherence in much the same way as they depend on spatial coherence. A detailed analysis should be developed. The production of holograms involving long optical path differences (such as shown by

Stetson and Powell[1]) seems to provide a promising avenue of experimentation.

REFERENCE

1. K. A. Stetson and R. L. Powell, J.Opt.Soc.Am.56, 1161 (1966).

APPENDIX I

AN EXPLANATION OF HOLOGRAPHY AS A MODULATION PROCESS

It is known in optics[1] that the distribution of radiation on a plane far from a source is the Fourier transform of that source distribution. Referring to Fig. AI-1 where S(x',y') is the amplitude distribution of the radiation from the source and H(x,y) is the resulting amplitude distribution on the plane H, we can write

$$H(x,y) = F\left[S(x',y')\right]$$

for infinite distance between S and H. Here, F denotes a Fourier transform. We are used to transformations between frequency and time; the transformations above are between spatial frequency and position. The illustrations in Fig. AI-2 demonstrate the analogy. This figure, however, shows only the amplitude of H(x,y), a complex quantity.

Clearly, if we could photographically record the distribution H(x,y), then some inverse transform process should reconstruct an image of the source S(x',y'). However, a photographic plate responds to the intensity of the incident radiation; we can assume for simplicity

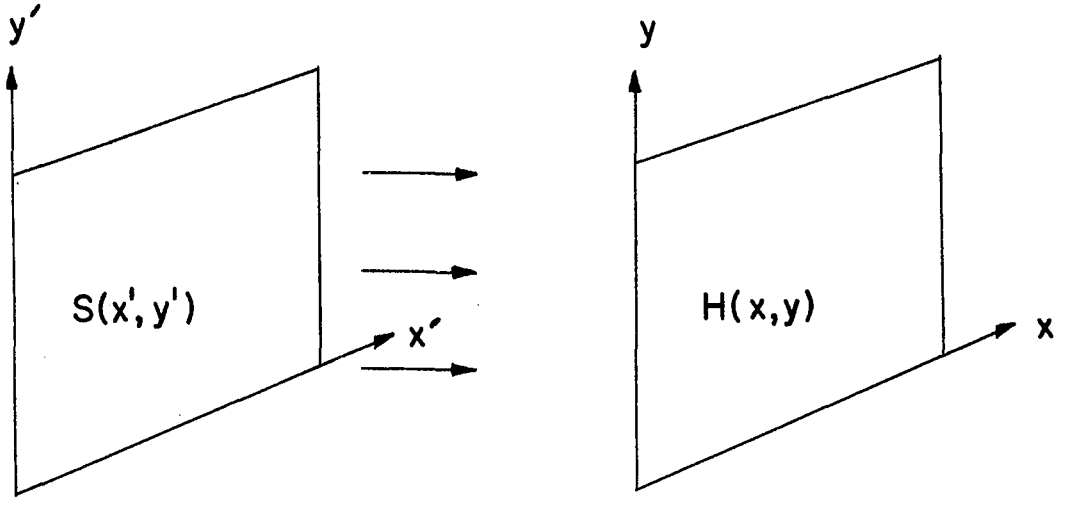

Figure AI-1. For infinite separation between the S and H planes, the radiation falling on H represents the Fourier transform of the radiation leaving S.

S PLANE

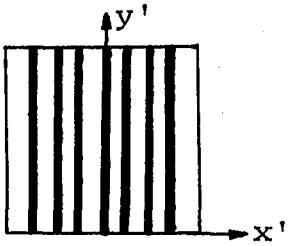

Spatial frequency of 8 cycles/inch in the x' direction. The amplitude of the radiation from the surface varies as $\sin 2\pi(8x')$.

H PLANE

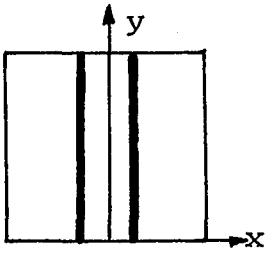

Spectrum has lines at $x = \pm 8$.

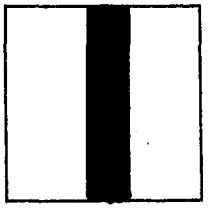

Square pulse in the x' direction. There is no radiation from the surface in the unshaded areas.

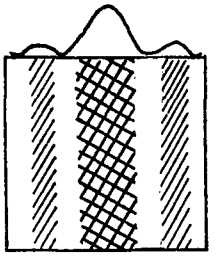

Spectrum of a square pulse.

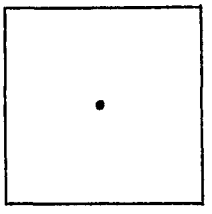

Impulse function (point source) in the x' and y' directions.

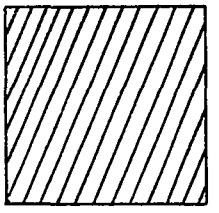

Spectrum of impulse; a uniform field of unit amplitude for all x and y.

Figure AI-2. Examples of spatial Fourier transforms. S(x',y') and H(x,y) are complex quantities; the figure shows only their magnitudes.

that the transmittance T(x,y) of the processed plate (for a positive) is proportional to the intensity of the light (see p. 43) or

$$T(x,y) \propto |H(x,y)|^2 \propto |F[S(x',y')]|^2 .$$

Therefore, the plate records the magnitude but not the phase of H(x,y) and information is lost. However, there is a procedure by means of which we can record both the amplitude and phase of $F[S(x',y')]$. Let us rotate the source S to form an angle α with the normal to the H plane, and at the same time, introduce a plane wave along the normal as in Fig. AI-3. The radiation on H, from S, will now be $F[S(x',y')]e^{jcx}$ where $c = \sin(2\pi\alpha/\lambda)$, while the radiation from the plane wave can be considered as having unit amplitude and zero phase.

With proper choice of origin for x, the transmittance of a photograph exposed as in Fig. AI-3 will be

$$T(x,y) \propto |F[S(x',y')]e^{jcx} + 1|^2 \qquad \text{(AI-1)}$$

$$\propto 1 + |F[S]|^2 + \underbrace{F[S]e^{jcx} + (F[S])^* e^{-jcx}}_{2|F[S]|\cos(\arg F[S] + cx)}.$$

The term under the horizontal bracket contains information about the magnitude and phase of S (through $F[S]$).

Now we must show that passing a plane wave through

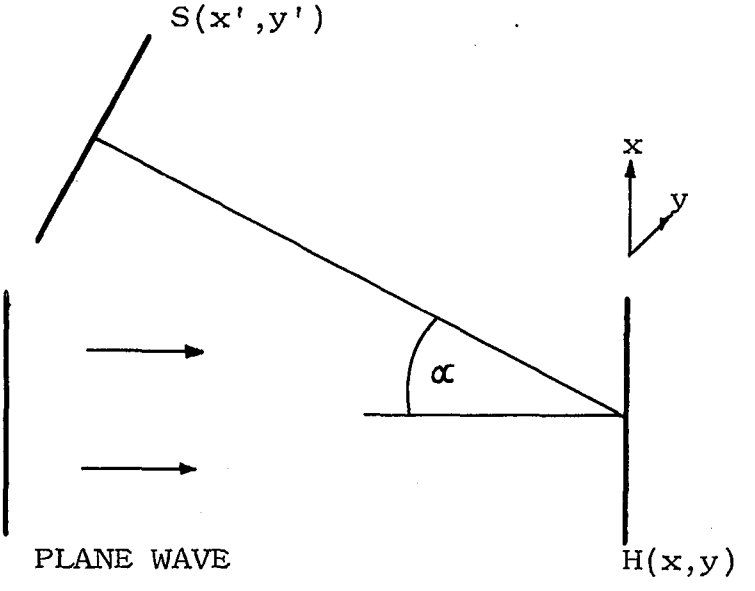

Figure AI-3. An arrangement for photographically recording the amplitude and phase of $F[S(x',y')]$ in the plane H. Such a photograph is a hologram.

the hologram whose transmittance is T(x,y) will reconstruct an image of the source S(x',y'). The wave leaving the illuminated hologram has the amplitude distribution T(x,y). As described on p. 122, this wave will produce a radiation distribution on a distant plane whose coordinates are x',y' given by

$$R(x',y') = F\left[T(x,y)\right].$$

The two terms in R(x',y') due to the last two terms in Eqn. AI-1 are

$$R_1(x',y') = F\left\{F\left[S(x',y')\right]e^{jcx}\right\}$$

and

$$R_2(x',y') = F\left\{F^*\left[S(x',y')\right]e^{-jcx}\right\} .$$

A little algebra yields

$$R_1(-x',-y') = F^{-1}\left\{F\left[S(x',y')\right]e^{jcx}\right\} = S(x'+c,y')$$

$$R_2(+x',y') = F\left\{F^{-1}\left[S(x',y')\right]e^{-jcx}\right\} = S(x'+c,y')$$

since, for real S(x',y'), $\left(F\left[S(x',y')\right]\right)^* = F^{-1}\left[S(x',y')\right]$. R_1 and R_2 are inverted, mirror(with respect to the x' axis) images in the x',y' plane.

Thus, we have shown that if a source S produces a hologram H, that hologram reconstructs two images, one of which is identical to S as illustrated in Fig. AI-4.

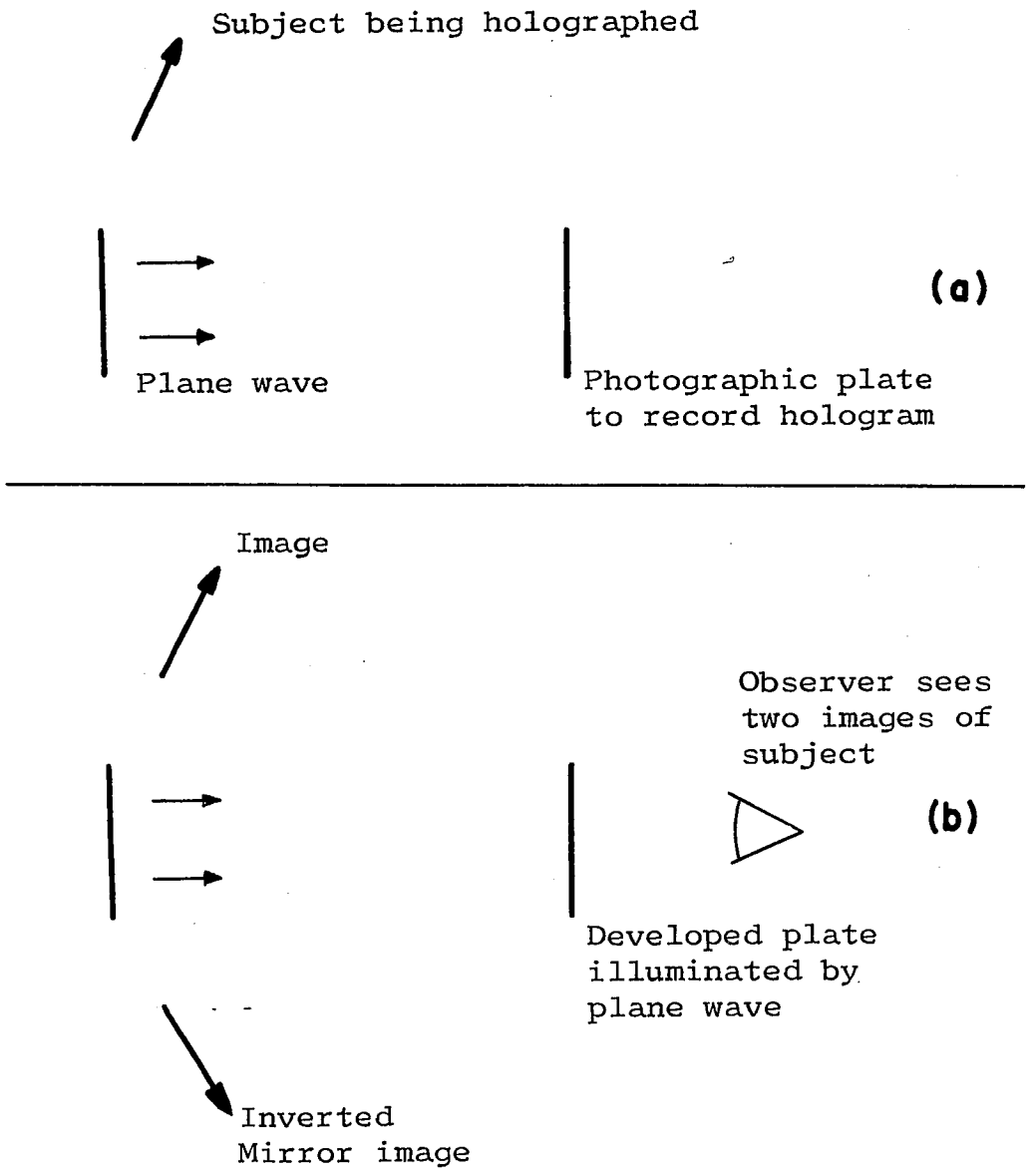

Figure AI-4. (a) Producing a hologram.

(b) Reconstructing the two images of the subject as explained in the text.

We have assumed above that the separation between the S and H planes, and the separation between the H and R planes, is very large. This assumption, which allowed us to use Fourier transforms, is not always met in practice. When the distance between the planes is finite, the same form of analysis applies, but more general, and more complicated, transform pairs are involved.

When the separation is very large, or when lenses are used to simulate infinite separation, the light leaving the hologram during the reconstruction process produces two images at infinity as described above. Holograms produced in this way are called Fourier transform holograms.[2] This type of hologram is characterized by the two mirror images in the reconstruction as indicated in Fig. AI-4. As the separations between the various planes are reduced, the beams to one image converge less (i.e. diverge), while the beams to the other converge more. Thus, in the usual type of hologram, one real image (formed by converging beams) and one virtual image (formed by diverging beams) is formed as shown in Chapter 1.

REFERENCES

1. M. Born and E. Wolf, Principles of Optics, 2d.ed., Pergamon Press, N. Y., 1964, p. 385.

2. G. W. Stroke, Brumm and Funkhouser, J.Opt.Soc.Am. 55, 1327 (1965).

APPENDIX II

A PHYSICAL EXPLANATION OF HOLOGRAM RECONSTRUCTION

An argument used by Bragg[1] to explain the early holograms produced by Gabor can be extended to the two beam Fresnel holograms receiving attention today. When one of these holograms is illuminated with a plane wave, it produces a three dimensional image of an object. This image is completely realistic (except that it is generally monochromatic) exhibits parallax, and requires the observer to refocus for near and distant objects. The following description of the hologram reconstruction process seems to provide somewhat greater physical insight than previous more mathematical descriptions[2,3].

A puzzling question about holograms is: how can one photographic plate reconstruct the complicated wavefront required to produce an image of a typical three dimensional object? The explanation lies in the fact that a hologram reconstructs not only a virtual image of the original object, but a conjugate image as well.

Reconstruction of the complicated wave emanating from a typical three dimensional object requires re-

cording and reproducing both amplitude and phase at some surface. However, a combination of the original object plus a conjugate image gives rise to a resultant wave that is simpler insofar as there exists in a certain position a wavefront which is plane.

More specifically, we will show that for any given three-dimensional object there exists a conjugate three-dimensional real image having the property that the diverging and converging waves associated with the pair combine to produce a plane wavefront somewhere in the system. In this plane the intensity distribution completely describes the wavefront since the phase is known to be constant. Therefore, a flat photographic plate having an appropriate transmittance distribution and illuminated by a plane wave can reconstruct this wavefront and, hence, the pair of three-dimensional images. Such a photograph is a hologram.

Consider the simple system indicated in Fig. AII-1, consisting of a point source of radiation O and a projector producing a real image O' of a similar point. The plane H, with coordinates x,y is equidistant from

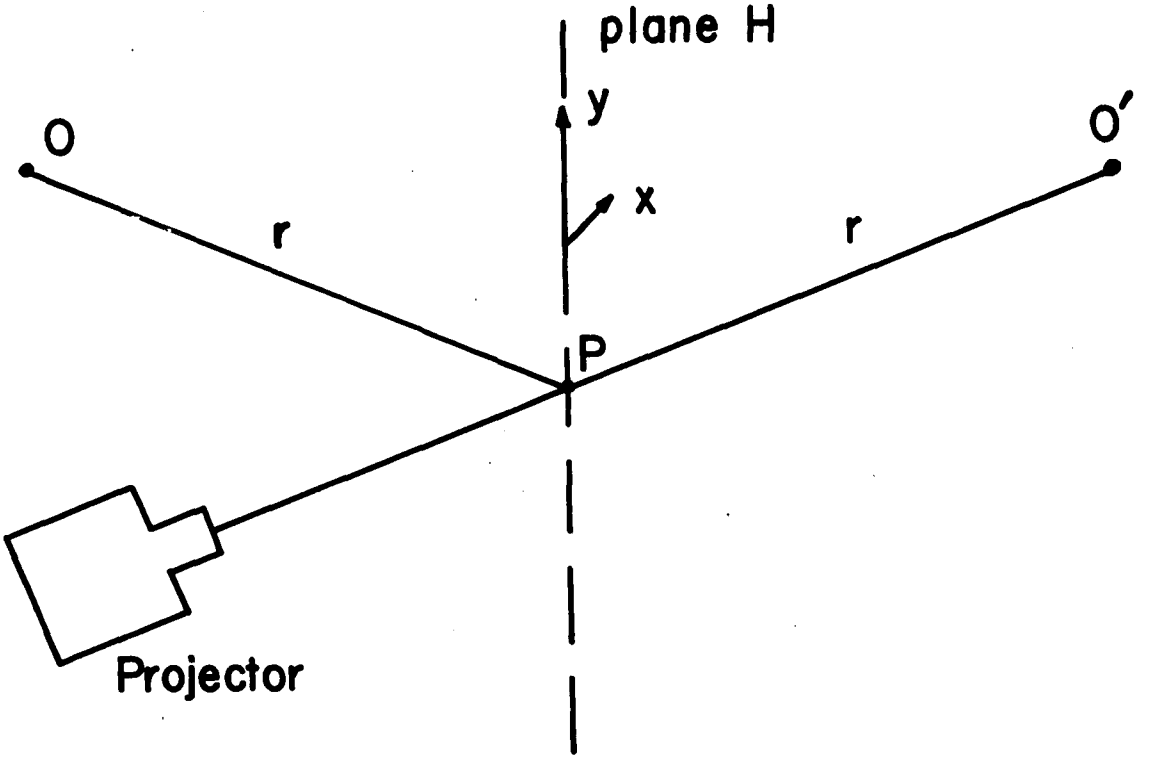

Figure AII-1. O is a point source of radiation and O' is a point image produced by the projector. As shown in the text, for appropriate phase relationships between O and O', there is a plane wavefront in the plane H.

O and O'. Let the radiation leaving O at time t be $a\cos(\omega t+\varphi)$; and let the radiation reaching O' at time t be $a\cos(\omega t-\varphi)$. An observer at the right of the diagram would see merely a point source and a point image since he is insensitive to phase. The analytic signal of the radiation from O that reaches a point P in the H plane at time t is $w_p = b(x,y)\cos(\omega t+\varphi-r/c)$; the analytic signal of the radiation from the projector that passes point P at time t, traveling to the image O', is $w'_p = b(x,y)\cos(\omega t-\varphi+r/c)$. Therefore, for this combination of source and image, the analytic signal at any point P on the plane H at time t is

$$W_p = w_p + w'_p = B(x,y)\cos\omega t \quad .$$

As the phase of this analytic signal is the same at all points on the plane H, this is a plane wavefront.

If O is an extended object emitting or reflecting coherent radiation and O' is an extended image such that corresponding points on O and O' are equidistant from the plane H as in Fig. AII-2, then the resultant analytic signal at the plane H has constant phase and some complicated amplitude distribution C(x,y). This again results in a plane wavefront. Each point of the image

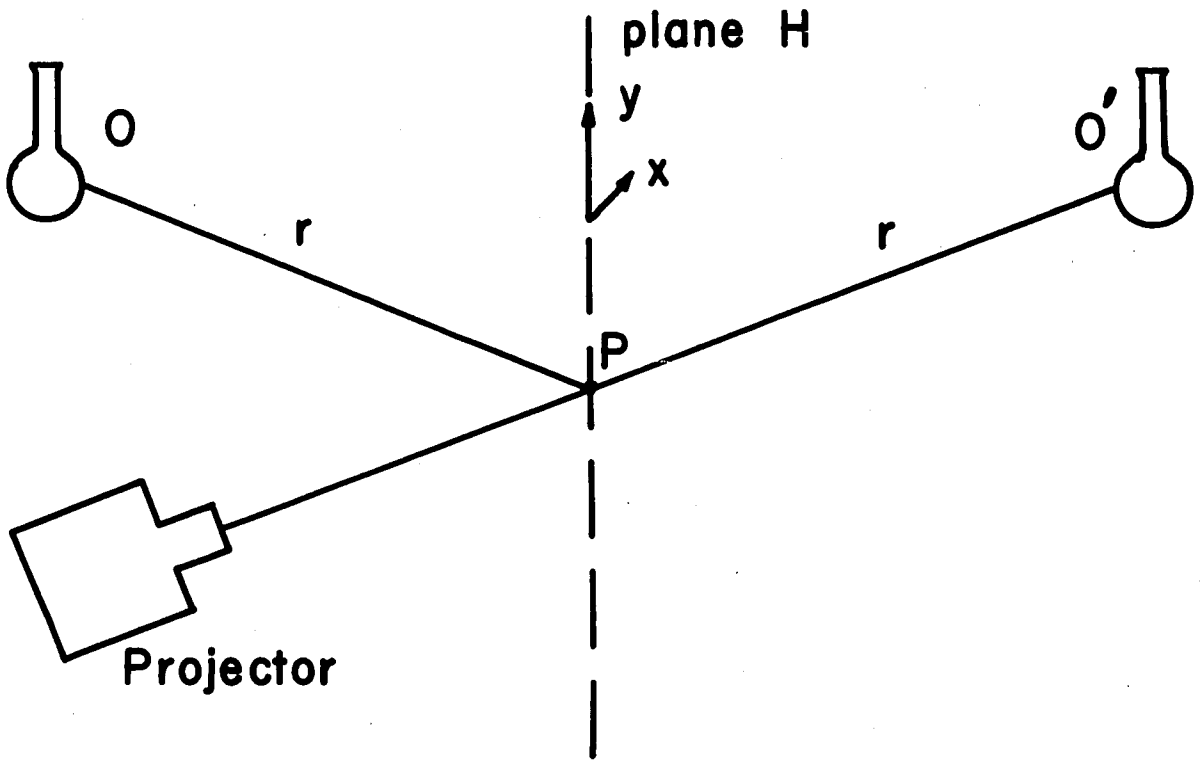

Figure AII-2. O is an extended, illuminated object and O' is an image produced by the projector of the form of a reflection of O in the plane H. For the appropriate phase relationships between the points on O and the corresponding points on O', there is a plane wavefront in the plane H.

O' is of the form of a reflection of the corresponding point on O with respect to the plane H.

Clearly, all the light reaching an observer at the right of either Fig. AII-1 or Fig. AII-2 must cross the plane H. There are two situations that are indistinguishable to such an observer:

1) the source and projector are both present as in Fig. AII-2,

and 2) neither is present, but there exists a wave traveling to the right, as in Fig. AII-3, having at H a wavefront described by $C(x,y)\cos\omega t$. (Notice that the phase is constant over all H.)

In particular, the observer sees the object O in both situations and, ideally, there is no optical test he can perform to determine whether the system is as described in Fig. AII-2 or AII-3.

The wavefront $C(x,y)\cos\omega t$ can be produced very simply by passing a plane wave of uniform amplitude through a transparency, a hologram, having an amplitude transmittance $C(x,y)$. This simple procedure will produce the

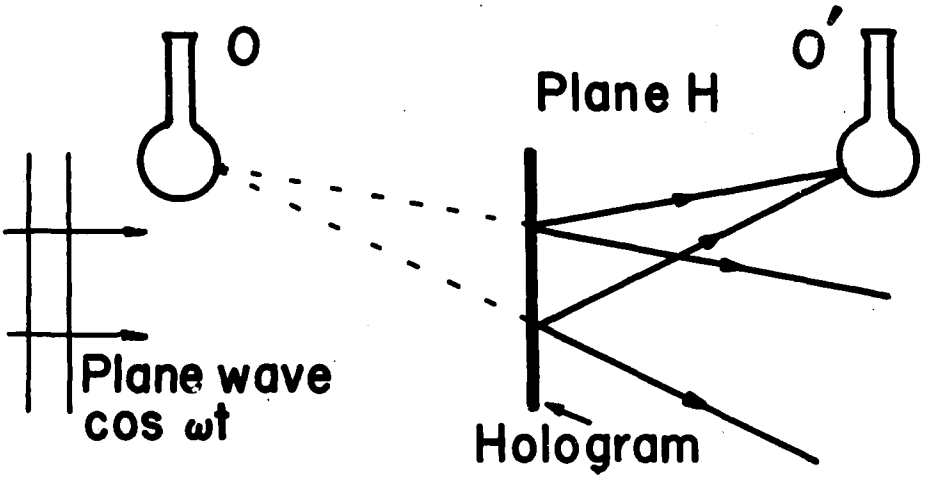

Figure AII-3. The plane H contains a transparency (hologram) with amplitude transmittance C(x,y). Therefore, the plane wavefront C(x,y)cosωt is reconstructed to the right of H. An observer seeing the resulting wave sees the two images O and O'.

pair of three-dimensional images O and O' from the single, flat transparency.

We conclude that a hologram does not really reconstruct the complicated wavefront associated with a three-dimensional object, but, rather reconstructs the much simpler plane wavefront associated with the object and an appropriate conjugate image.

REFERENCES

1. W. L. Bragg, Nature 166, 399 (1950).

2. E. Leith and J. Upatnieks, J.Opt.Soc.Am. 53, 1377 (1963).

3. E. Leith and J. Upatnieks, J.Opt.Soc.Am. 54, 1295 (1964).

REFERENCES

M. J. Beran and G. B. Parrent, Jr., Theory of Partial Coherence, Prentice Hall, N. J., 1964.

M. Born and E. Wolf, Principles of Optics 2d. ed., Pergamon Press, N. Y., 1964.

W. L. Bragg, Nature 166, 399 (1950).

W. B. Davenport, Jr. and W. L. Root, An Introduction to the Theory of Random Signals and Noise, McGraw-Hill, N. Y., 1958.

D. Gabor, Nature 161, 777 (1948).

D. Gabor, Nature 162, 764 (1948).

E. Jahnke and G. Emde, Tables of Functions, Dover Publications, N. Y., 1945.

F. A. Jenkins and H. E. White, Fundamentals of Optics, McGraw-Hill, N. Y., 1957.

P. Kirkpatrick and H. M. A. El-Sum, J.Opt.Soc.Am. 46, 825 (1956).

E. Leith and J. Upatnieks, J.Opt.Soc.Am. 52, 1123 (1962).

E. Leith and J. Upatnieks, J.Opt.Soc.Am. 53, 1377 (1963).

E. Leith and J. Upatnieks, J.Opt.Soc.Am. 54, 1295 (1964).

M. Lurie, J.Opt.Soc.Am. 56, 1369 (1966).

L. Mandel and E. Wolf, Rev. Mod. Phys. 37, 231 (1965).

R. W. Meier, J.Opt.Soc.Am. 55, 987 (1965).

R. L. Powell and K. A. Stetson, J.Opt.Soc.Am. 55, 1593 (1965).

K. A. Stetson and R. L. Powell, J.Opt.Soc.Am. 56, 1161 (1966).

G. W. Stroke, D. Brumm and A. Funkhouser, J.Opt.Soc.Am. 55, 1327 (1965).

P. H. van Cittert, Physica 1, 201 (1934).

J. T. Winthrop and C. R. Worthington, Phys. Letters 15, 124, (1965).

F. Zernike, Physica 5, 785 (1938).

The International Dictionary of Physics and Electronics, 2d. ed., D. Van Nostrand Co., Inc., N. J., 1961.

VITA

1959 B. S. (Physics), Brooklyn College, Brooklyn, N.Y.

1961 M. S. (Physics), Rutgers University, New Brunswick, N. J.

Professional Background

1959-61 Teaching and Research Assistant, Rutgers.

1961-63 Physicist, Gulton Industries, Inc., Metuchen, N.J.

1963-65 Assistant Instructor, Newark College of Engineering, Newark, N. J.

1965-66 Research Fellow, Newark College of Engineering.

1966-67 Instructor, Newark College of Engineering.

This research was conducted at Newark College of Engineering during the years 1965 - 1967.